

# The idiots guide to Quantum Error Correction.

Simon J. Devitt\* and Kae Nemoto

*National Institute of Informatics, 2-1-2 Hitotsubashi, Chiyoda-ku, Tokyo 101-8340, Japan.*

William J. Munro

*Hewlett-Packard Laboratories, Filton Road, Stoke Gifford, Bristol BS34 8QZ, UK and  
National Institute of Informatics, 2-1-2 Hitotsubashi, Chiyoda-ku, Tokyo 101-8430, Japan*

(Dated: May 27, 2022)

Quantum Error Correction and fault-tolerant quantum computation represent arguably the most vital theoretical aspect of quantum information processing. It was well known from the early developments of this exciting field that the fragility of coherent quantum systems would be a catastrophic obstacle to the development of large scale quantum computers. The introduction of Quantum Error Correction in 1995 showed that active techniques could be employed to mitigate this fatal problem. However, Quantum Error Correction and fault-tolerant computation is now a much more mature field and many new codes, techniques and methodologies have been developed to implement error correction for large scale quantum algorithms. This development has been so pronounced that many in the field of quantum information, specifically those new to quantum information or those focused on the many other important issues in quantum computation have not been able to keep up with the general formalisms and methodologies employed in this area. In response we have attempted to summarize the basic aspects of Quantum Error Correction and fault-tolerance, not as a detailed guide, but rather as a basic introduction. Rather than introducing these concepts from a rigorous mathematical and computer science framework, we instead examine error correction and fault-tolerance largely through detailed examples, progressing from basic examples of the 3-qubit code through to the stabilizer formalism which is now extremely important when understanding large scale concatenated code structures, quantum circuit synthesis and the more recent developments in subsystem and topological codes.

PACS numbers: 03.67.Lx, 03.67.Pp

## Contents

<b>I. Introduction</b>	1	<b>C. More General mappings</b>	17
<b>II. Preliminaries</b>	3	<b>X. fault-tolerant Quantum Error Correction and the threshold theorem.</b>	17
<b>III. Quantum Errors: Cause and Effect</b>	3	A. Fault-tolerance	17
A. Coherent Quantum Errors: You don't know what you are doing!	4	B. Threshold Theorem	18
B. Decoherence: The devil is in the environment	4	<b>XI. fault-tolerant operations on encoded data</b>	18
C. Loss, Leakage, Measurement and Initialization: Variations of the above	5	A. Single Qubit Operations	19
<b>IV. QEC, a good starting point: The 3-qubit code</b>	6	B. Two-qubit gate.	20
<b>V. The Nine Qubit Code: The First Full Quantum code</b>	9	<b>XII. fault-tolerant circuit design for logical state preparation</b>	21
<b>VI. Quantum Error Detection</b>	10	<b>XIII. Loss Protection</b>	22
<b>VII. Stabilizer Formalism</b>	11	<b>XIV. Some Modern Developments in Error Correction</b>	26
<b>VIII. QEC with stabilizer codes</b>	12	A. Subsystem Codes	26
A. State Preparation	13	B. Topological Codes	29
B. Error Correction	14	<b>XV. Conclusions and future outlook</b>	31
<b>IX. Digitization of Quantum Errors</b>	15	<b>XVI. Acknowledgments</b>	33
A. Systematic gate errors	15	<b>References</b>	33
B. Environmental decoherence	15	<b>I. INTRODUCTION</b>	

\*electronic address: devitt@nii.ac.jp

The micro-computer revolution of the late 20th century has arguably been of greater impact to the world than any other technological revolution in history. The advent of

transistors, integrated circuits, and the modern microprocessor has spawned literally hundreds of devices from pocket calculators to the iPod, all now integrated through an extensive worldwide communications system. However, as we enter the 21st century, the rate at which computational power is increasing is driving us very quickly to the realm of quantum physics. The component size of individual transistors on modern microprocessors are becoming so small that quantum effects will soon begin to dominate over classical electronic properties. Unfortunately the current designs for micro-electronics mean that quantum mechanical behavior will tend to result in unpredictable and unwanted behavior. Therefore, we have two choices: to keep trying to suppressing quantum effects in classically fabricated electronics or move to the field of quantum information processing (QIP) where we instead exploit them. This leads to a paradigm shift in the way we view and process information and has lead to considerable interest from physicists, engineers, computer scientists and mathematicians. The counter-intuitive and strange rules of quantum physics offers enormous possibilities for information processing and the development of a large scale quantum computer is the holy grail of many groups worldwide.

While the advent of Shor's algorithm (Sho97) certainly spawned great interest in quantum information processing and demonstrated that the utilization of a quantum computer could lead to algorithms far more efficient than those used in classical computing, there was a great deal of debate surrounding the practicality of building a large scale, controllable, quantum system. It was well known even before the introduction of quantum information that coherent quantum states were extremely fragile and many believed that to maintain large, multi-qubit, coherent quantum states for a long enough time to complete *any* quantum algorithm was unrealistic (Unr95). Additionally, classical error correction techniques are intrinsically based on a digital framework. Hence, can the vast amount of knowledge gained from classical coding theory be adapted to the quantum regime where while the *readout* of qubits is digital but actual manipulations are analogue.

Starting in 1995, several papers appeared, in rapid succession, proposing codes which were appropriate to perform error correction on quantum data (Sho95; Ste96a; CS96; LMPZ96). This was the last theoretical aspect needed to convince the general community that quantum computation was indeed a possibility. Since this initial introduction, the progress in this field has been extensive.

Initial work on error correction focused heavily on developing quantum codes (Ste96b; CG97; Got96; PVK97), introducing a more rigorous theoretical framework for the structure and properties of Quantum Error Correction (QEC) (KL00; CRSS98; Gro97; KLV00; KLP05) and the introduction of concepts such as fault-tolerant quantum computation (Sho96; DS96; Got98) which leads directly to the threshold theorem for concatenated QEC (KLZ96; ABO97). In more recent years QEC pro-

ocols have been developed for various systems, such as continuous variables (LS98; Bra98; vL08; ATK<sup>+</sup>08), ion-traps and other systems containing motional degrees of freedom (LW03b; ST98), adiabatic computation (JFS06) and globally controlled quantum computers (BBK03). Additionally, work still continues on not only developing more complicated (and in some ways, more technologically useful) protocols such as subsystem codes (Bac06) and topological codes (Kit97; DKLP02; RHG07; FSG08) but also advanced techniques to implement error correction in a fault-tolerant manner (Ste97a; Ste02; DA07).

Along with QEC, other methods of protecting quantum information were also developed. These other techniques would technically be placed in a separate category of error avoidance rather than error correction. The most well known technique of error avoidance is protocols such as decoherence free subspaces (DFS) (DG97; DG98b; ZR97b; ZR97a; DG98a; LW03a). While this protocol has the mathematical structure of a self correcting quantum code, it is largely a technique to suppress certain, well structured, noise models. As with QEC, this field of error avoidance is vast, now incorporating ideas from optimal control to create specially designed control sequences to counteract the effect of errors induced from environmental coupling. These new methods of dynamical decoupling can take simple structures such as Bang-Bang control (VL98; VT99; Zan99), to more complicated and generalized protocols to help decouple qubits from the environment (VKL99; FLP04; VK03; VK05).

This review deals exclusively with the concepts of QEC and fault-tolerant quantum computation. Many papers have reviewed error correction and Fault-tolerance (Got97; NC00; Got02; KLA<sup>+</sup>02; Ste01; Got09), however to cater for a large audience, we attempt to describe QEC and Fault-tolerance in a much more basic manner, largely through examples. Instead of providing a more rigorous review of error correction, we instead try to focus on more practical issues involved when working with these ideas. For those who have recently begun investigating quantum information processing or those who are focused on other important theoretical and/or experimental aspects related to quantum computing, searching through this enormous collection of work is daunting especially if a basic working knowledge of QEC is all that is required. We hope that this review of the basic aspects of QEC and fault-tolerance will allow those with little knowledge of the field to quickly become accustomed to the various techniques and tricks that are commonly used.

We begin the discussion in section II where we share some preliminary thoughts on the required properties of any quantum error correcting protocol. In section III we review some basic noise models from the context of how they influence quantum algorithms. Section VII introduces quantum error correction through the traditional example of the 3-qubit code, illustrating the circuits used for encoding and correction and why the principal of redundant encoding suppresses the failure of en-

coded qubits. Section VII then introduces the stabilizer formalism (Got97), demonstrating how QEC circuits are synthesized once the structure of the code is known. In section IX we then briefly return to the noise models and relate the abstract analysis of QEC, where errors are assumed to be discrete and probabilistic, to some of the physical mechanisms which can cause errors. Sections X and XI introduces the concept of fault-tolerant error correction, the threshold theorem and how logical gate operations can be applied directly to quantum data. We then move on to circuit synthesis in section XII presenting a basic fault-tolerant circuit design for logical state preparation using the  $[[7,1,3]]$  Steane code as a representative example of how to synthesize fault-tolerant circuits from the stabilizer structure of quantum codes. Finally in section XIV we review specific codes for qubit loss and examine two of the more modern techniques for error correction. We briefly examine quantum subsystem codes (Bac06) and topological surface codes (DKLP02; FSG08) due to both their theoretical elegance and their increasing relevance in quantum architecture designs (DFS<sup>+</sup>08).

## II. PRELIMINARIES

Before discussing specifically the effect of errors and the basics of Quantum Error Correction (QEC) we first dispense with the very basics of qubits and quantum gates. We assume a basic working knowledge with quantum information (EJ96; NC00) and this brief discussion is used simply to define our notation for the remainder of this review.

The fundamental unit of quantum information, the qubit, which unlike classical bits can exist in coherent superpositions of two states, denoted  $|0\rangle$  and  $|1\rangle$ . These basis states can be photonic polarization, spin states, electronic states of an ion or charge states of superconducting systems. An arbitrary state of an individual qubit,  $|\phi\rangle$ , can be expressed as,

$$|\phi\rangle = \alpha|0\rangle + \beta|1\rangle \quad (1)$$

where normalization requires,  $|\alpha|^2 + |\beta|^2 = 1$ . Quantum gate operations are represented by unitary operations acting on the Hilbert space of a qubit array. Unlike classical information processing, conservation of probability for quantum states require that all operations be reversible and hence unitary.

When describing a quantum gate on an individual qubit, any dynamical operation,  $G$ , is a member of the unitary group  $U(2)$ , which consists of all  $2 \times 2$  matrices where  $G^\dagger = G^{-1}$ . Up to a global (and unphysical) phase factor, any single qubit operation can be expressed as a linear combination of the generators of  $SU(2)$  as,

$$G = c_I \sigma_I + c_x \sigma_x + c_y \sigma_y + c_z \sigma_z \quad (2)$$

where,

$$\sigma_x = \begin{pmatrix} 0 & 1 \\ 1 & 0 \end{pmatrix}, \quad \sigma_y = \begin{pmatrix} 0 & -i \\ i & 0 \end{pmatrix}, \quad \sigma_z = \begin{pmatrix} 1 & 0 \\ 0 & -1 \end{pmatrix}, \quad (3)$$

are the Pauli matrices,  $\sigma_I$  is the  $2 \times 2$  identity matrix and the co-efficients  $(c_I, c_x, c_y, c_z) \in \mathcal{C}$  satisfy  $|c_I|^2 + |c_x|^2 + |c_y|^2 + |c_z|^2 = 1$ .

The concept of Quantum Error Correction (QEC) is fundamental to the large scale viability of quantum information processing. Although the field is largely based on classical coding theory, there are several issues that need to be considered when transferring classical error correction to the quantum regime.

First, coding based on data-copying, which is extensively used in classical error correction cannot be used due to the no-cloning theorem of quantum mechanics (WZ82). This result implies that there exists no transformation resulting in the following mapping,

$$U|\phi\rangle \otimes |\psi\rangle = |\phi\rangle \otimes |\phi\rangle. \quad (4)$$

i.e. it is impossible to perfectly copy an unknown quantum state. This means that quantum data cannot be protected from errors by simply making multiple copies. Secondly, direct measurement cannot be used to effectively protect against errors, since this will act to destroy any quantum superposition that is being used for computation. Error correction protocols must therefore be employed which can detect and correct errors without determining *any* information regarding the qubit state. Finally, unlike classical information, qubits can experience traditional bit errors,  $|0\rangle \leftrightarrow |1\rangle$  but unlike classical information, qubit are also susceptible to phase errors  $|1\rangle \leftrightarrow -|1\rangle$ . Hence any error correcting procedure needs to be able to simultaneously correct for both.

At its most basic level, QEC utilizes the idea of redundant encoding where quantum data is protected by extending the size of the Hilbert space for a single, logically encoded qubit and essentially spreading out the information over multiple qubits. This way, errors only perturb codeword states by small amounts which can then be detected and corrected, without directly measuring the quantum state of any qubit.

## III. QUANTUM ERRORS: CAUSE AND EFFECT

Before we even begin discussing the details of quantum error correction, we first examine some of the common sources of errors in quantum information processing and contextualize what they imply for computation. We will consider several important sources of errors and how they influence a trivial, single qubit, quantum algorithm.

This trivial algorithm will be a computation consisting of a single qubit, initialized in the  $|0\rangle$  state undergoing  $N$  identity operations. Such that the final, error free state is,

$$|\psi\rangle_{\text{final}} = \prod_{i=1}^N \sigma_I |0\rangle = |0\rangle, \quad (5)$$

Measurement of the qubit in the  $|0\rangle, |1\rangle$  basis will consequently yield the result 0 with a probability of unity. We examine, independently, several common sources of error from the effect they have on this simple quantum algorithm. Hopefully, this introductory section will show that while quantum errors are complicated physical effects, in QIP the relevant measure is the theoretical success probability of a given quantum algorithm.

### A. Coherent Quantum Errors: You don't know what you are doing!

The first possible source of error is coherent, systematic control errors. This type of error is typically associated with bad system control and/or characterization where imprecise manipulation of the qubit introduces inaccurate Hamiltonian dynamics. As this source of error is produced by inaccurate control of the system dynamics it does not produce mixed states from pure states (i.e. it is a coherent, unitary error and does not destroy the quantum coherence of the qubit but instead causes you to apply an undesired gate operation). In our trivial algorithm, we are able to model this several different ways. To keep things simple, we assume that incorrect characterization of the control dynamics leads to an identity gate which is not  $\sigma_I$ , but instead introduces a small rotation around the  $X$ -axis of the Bloch sphere, i.e.

$$|\psi\rangle_{\text{final}} = \prod_{x=1}^N e^{i\epsilon\sigma_x} |0\rangle = \cos(N\epsilon) |0\rangle + i \sin(N\epsilon) |1\rangle. \quad (6)$$

We now measure the system in the  $|0\rangle$  or  $|1\rangle$  state. In the ideal case, the computer should collapse to the state  $|0\rangle$  with a probability of one,  $P(|0\rangle) = 1$ . However we now find,

$$\begin{aligned} P(|0\rangle) &= \cos^2(N\epsilon) \approx 1 - (N\epsilon)^2, \\ P(|1\rangle) &= \sin^2(N\epsilon) \approx (N\epsilon)^2. \end{aligned} \quad (7)$$

Hence, the probability of error in this trivial quantum algorithm is given by  $p_{\text{error}} \approx (N\epsilon)^2$ , which will be small given that  $N\epsilon \ll 1$ . The systematic error in this system is proportional to both the small systematic over rotation and the total number of applied identity operations.

### B. Decoherence: The devil is in the environment

Environmental decoherence is another important source of errors in quantum systems. Once again we will take a very basic example of a decoherence model and examine how it influences our trivial algorithm. Later in section IX we will illustrate a more complicated decoherence model that arises from standard mechanisms.

Consider a very simple environment, which is another two level quantum system. This environment has two basis states,  $|e_0\rangle$  and  $|e_1\rangle$  which satisfies the completeness relations,

$$\langle e_i | e_j \rangle = \delta_{ij}, \quad |e_0\rangle \langle e_0| + |e_1\rangle \langle e_1| = I. \quad (8)$$

We will also assume that the environment couples to the qubit in a specific way. When the qubit is in the  $|1\rangle$  state, the coupling flips the environmental state while if the qubit is in the  $|0\rangle$  state nothing happens to the environment. Additionally, as we anticipate the effect of this decoherence model we will slightly alter our trivial algorithm. Rather than considering a qubit prepared in the  $|0\rangle$  state and applying  $N$  identity operations, we instead modify the algorithm to the following,

$$\begin{aligned} |\psi\rangle_{\text{final}} &= H\sigma_I H |0\rangle = H\sigma_I \frac{1}{\sqrt{2}}(|0\rangle + |1\rangle) \\ &= H \frac{1}{\sqrt{2}}(|0\rangle + |1\rangle) = |0\rangle. \end{aligned} \quad (9)$$

Essentially we are performing two  $H \equiv$  Hadamard operations separated by a wait stage, represented by the Identity gate. Finally, this model assumes the system/environment interaction only occurs during this wait stage of the algorithm. As with the previous algorithm we should measure the state  $|0\rangle$  with probability one. The reason for modifying our trivial algorithm is because this specific decoherence model acts to reduce coherence between the  $|0\rangle$  and  $|1\rangle$  basis states and hence we require a coherent superposition to observe any effect from the environmental coupling.

We now assume that the environment starts in the pure state,  $|E\rangle = |e_0\rangle$ , and couples to the system such that,

$$H\sigma_I H |0\rangle |E\rangle = \frac{1}{2}(|0\rangle + |1\rangle) |e_0\rangle + \frac{1}{2}(|0\rangle - |1\rangle) |e_1\rangle \quad (10)$$

As we are considering environmental decoherence, pure states will be transformed into classical mixtures, hence we now move into the density matrix representation for the state  $H\sigma_I H |0\rangle |E\rangle$ ,

$$\begin{aligned} \rho_f &= \frac{1}{4}(|0\rangle \langle 0| + |0\rangle \langle 1| + |1\rangle \langle 0| + |1\rangle \langle 1|) |e_0\rangle \langle e_0| \\ &\quad + \frac{1}{4}(|0\rangle \langle 0| - |0\rangle \langle 1| - |1\rangle \langle 0| + |1\rangle \langle 1|) |e_1\rangle \langle e_1| \\ &\quad + \frac{1}{4}(|0\rangle \langle 0| - |0\rangle \langle 1| + |1\rangle \langle 0| - |1\rangle \langle 1|) |e_0\rangle \langle e_1| \\ &\quad + \frac{1}{4}(|0\rangle \langle 0| + |0\rangle \langle 1| - |1\rangle \langle 0| - |1\rangle \langle 1|) |e_1\rangle \langle e_0|. \end{aligned} \quad (11)$$

Since we do not measure the environmental degrees of freedom, we trace over this part of the system, giving,

$$\begin{aligned} \text{Tr}_E(\rho_f) &= \frac{1}{4}(|0\rangle \langle 0| + |0\rangle \langle 1| + |1\rangle \langle 0| + |1\rangle \langle 1|) \\ &\quad + \frac{1}{4}(|0\rangle \langle 0| - |0\rangle \langle 1| - |1\rangle \langle 0| + |1\rangle \langle 1|) \\ &= \frac{1}{2}(|0\rangle \langle 0| + |1\rangle \langle 1|). \end{aligned} \quad (12)$$

Measurement of the system will consequently return  $|0\rangle$  50% of the time and  $|1\rangle$  50% of the time. This final state is a complete mixture of the qubit states and is consequently a classical system. The coupling to the environment removed all the coherence between the  $|0\rangle$  and  $|1\rangle$

states and consequently the second Hadamard transform, intended to rotate  $(|0\rangle + |1\rangle)/\sqrt{2} \rightarrow |0\rangle$  has no effect.

Since we assumed that the system/environment coupling during the wait stage causes the environmental degree of freedom to “flip” when the qubit is in the  $|1\rangle$  state, this decoherence model implicitly incorporates a temporal effect. The temporal interval of our identity gate in the above algorithm is long enough to enact this full controlled-flip operation. If we assumed a controlled rotation that is not a full flip on the environment, the final mixture will not be 50/50. Instead there would be a residual coherence between the qubit states and an increased probability of our algorithm returning a  $|0\rangle$ . Section IX revisits the decoherence model and illustrates how time-dependence is explicitly incorporated.

### C. Loss, Leakage, Measurement and Initialization: Variations of the above

Other sources of error such as qubit initialization, measurement errors, qubit loss and qubit leakage are modeled in a very similar manner. Measurement errors and qubit loss are modeled in the same way as environmental decoherence. Measurement errors are described by utilizing the following measurement projection onto a qubit space,

$$A = (1 - p_M) |0\rangle \langle 0| + p_M |1\rangle \langle 1| \quad (13)$$

where  $p_M \in [0, 1]$  is the probability of measurement error. If we have a pure state  $\rho = |0\rangle \langle 0|$ , the probability of measuring a  $|0\rangle$  is,

$$P(|0\rangle) = \text{Tr}(A\rho) = (1 - p) \quad (14)$$

indicating that the correct result is observed with probability  $1 - p$ .

Qubit loss is modeled in a slightly similar manner. When a qubit is lost, it is essentially coupled to the environment which acts to measure the system, with the classical information lost. This coupling follows the decoherence analysis shown earlier, where a 50/50 mixed state of the qubit results. Therefore the projector onto the qubit space is given by  $A = \frac{1}{2}(|0\rangle \langle 0| + |1\rangle \langle 1|)$ , which is identical to simply tracing over the lost qubit and equivalent to a measurement error of probability  $p = 0.5$ . With this type of error channel, not only is the physical object lost (and hence cannot be directly measured), but an initially pure qubit is converted to a completely mixed state. While this model of qubit loss is equivalent to environmental coupling, correcting this type of error requires additional machinery on top of standard QEC protocols. The difficulty with qubit loss is the initial detection of whether the qubit is actually present. While standard correction protocols can protect against the loss of information on a qubit, this still assumes that the physical object still exists in the computer. Hence in loss correction protocols, an initial non-demolition detection method must be employed (which determines if

the qubit is actually present without performing a projective measurement on the computational state) before standard correction can be utilized to correct the error.

Initialization of the qubit can be modeled either using a coherent systematic error model or using the decoherence model. The specific methodology depends largely on the physical mechanisms used to initialize the system. If a decoherence model is employed, initialization is modeled exactly the same way as imperfect measurement. If we have a probability  $p_I$  of initialization error, the initial state of the system is given by the mixture,

$$\rho_i = (1 - p_I) |0\rangle \langle 0| + p_I |1\rangle \langle 1|. \quad (15)$$

In contrast, we could consider an initialization model which is achieved via a coherent unitary operation where the target is the desired initial state. In this case, the initial state is pure, but contains a non-zero amplitude of the undesired target, for example,

$$|\psi\rangle_i = \alpha |0\rangle + \beta |1\rangle \quad (16)$$

where  $|\alpha|^2 + |\beta|^2 = 1$  and  $|\beta|^2 \ll 1$ . The interpretation of these two types of initialization models is identical to the coherent and incoherent models presented. Again, the effect of these types of errors relates to the probabilities of measuring the system in an erred state.

One final type of error that we can briefly mention is the problem of qubit leakage. Qubit leakage manifests itself due to the fact that most systems utilized for qubit applications are not simple two level quantum systems. For example, Fig 1 (from Ref. (Ste97b)) illustrates the energy level structure for a  $^{43}\text{Ca}^+$  ion utilized for ion trap quantum computing at Oxford. The qubit in this system is defined only with two electronic states, however the system itself contains many more levels (including some which are used for qubit readout and initialization through optical pumping and photo-luminescence). As with systematic errors, leakage can occur when improper control is applied to such a system. In the case of ion-traps, qubit transitions are performed by focusing finely tuned lasers resonant on the relevant transitions. If the laser frequency fluctuates or additional levels are not sufficiently detuned from the qubit resonance, the following transformation could occur,

$$U|0\rangle = \alpha |0\rangle + \beta |1\rangle + \gamma |2\rangle, \quad (17)$$

where the state  $|2\rangle$  is a third level which is now populated due to improper control. The actual effect of this type of error can manifest in several different ways. The primary problem with leakage is that it violates the basic assumption of a qubit structure to the computer. As quantum circuits and algorithms are fundamentally designed assuming the computational array is a collection of 2-level systems, operators of the above form (which in this case is operating over a 3-level space) will naturally induce unwanted dynamics. Another important implication of applying non-qubit operations is how these levels interact with the environment and hence how decoherence

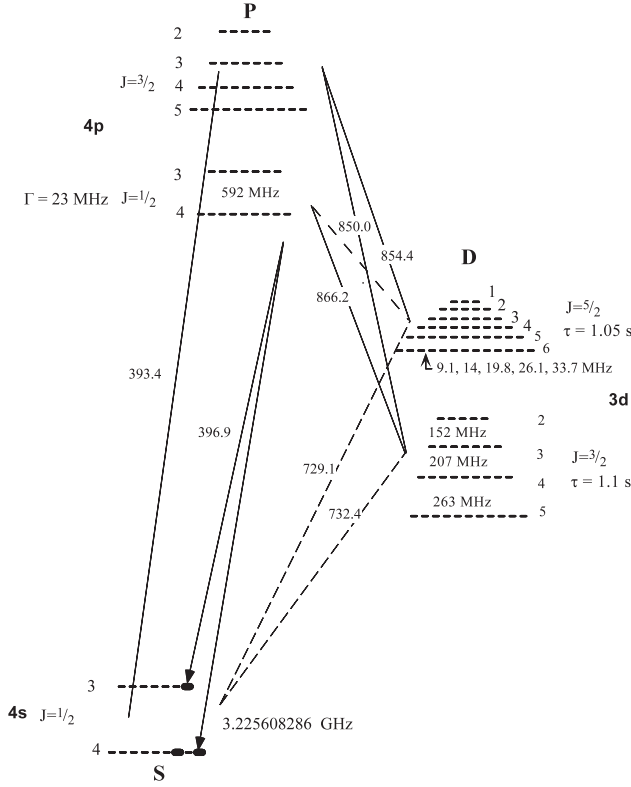


FIG. 1 (from Ref. (Ste97b)) Energy level structure for the  $^{43}\text{Ca}^+$  investigated by the Oxford ion-trapping group. The structure of this ion is clearly not a 2-level quantum system. Hence leakage into non-qubit states is an important factor to consider.

effects the system. For example, in the above case, the unwanted level,  $|2\rangle$ , may be extremely short lived leading to an emission of a photon and the system relaxing back to the ground state. For these reasons, leakage is one of the most problematic error channels to correct using QEC. In general, leakage induced errors need to be corrected via the non-demolition detection of a leakage event (i.e. determining if the quantum system is confined to a qubit without performing a measurement discriminating the  $|0\rangle$  and  $|1\rangle$  states (Pre98; GBP97; VWW05)) or through the use of complicated pulse control which acts to re-focus a improperly confined quantum gate back to the qubit subspace (WBL02; BLWZ05). In the context of mass manufacturing of qubit systems, leakage would be quantified immediately after the fabrication of a device, using intrinsic characterization protocols such as those discussed in Ref. (DSO<sup>+</sup>07). If a particular system is found to be improperly confined to the qubit subspace it

would simply be discarded. Employing characterization at this stage would then eliminate the need to implement pulse control of leakage, shortening gate times and ultimately reducing error rates in the computer.

In this section we introduced the basic ideas of quantum errors and how they effect the success of a quantum algorithm. Section IX will return in a more focused manner to error models and how they relate to error correction in a quantum computer.

#### IV. QEC, A GOOD STARTING POINT: THE 3-QUBIT CODE

The 3-qubit bit-flip code is traditionally used as a basic introduction to the concept of Quantum Error Correction. However, it should be emphasized that the 3-qubit code *does not* represent a full quantum code. This is due to the fact that the code cannot simultaneously correct for both bit and phase flips (see section. IX), which is a sufficient condition for correcting errors for an arbitrary error mapping on a single qubit. This code is a standard repetition code which was extended by Shor (Sho95) to the full 9-qubit quantum code which was the first demonstration that QEC was possible.

The 3-qubit code encodes a single logical qubit into three physical qubits with the property that it can correct for a single  $\sigma_x \equiv X$  bit-flip error. The two logical basis states  $|0\rangle_L$  and  $|1\rangle_L$  are defined as,

$$|0\rangle_L = |000\rangle, \quad |1\rangle_L = |111\rangle, \quad (18)$$

such that an arbitrary single qubit state  $|\psi\rangle = \alpha|0\rangle + \beta|1\rangle$  is mapped to,

$$\begin{aligned} \alpha|0\rangle + \beta|1\rangle &\rightarrow \alpha|0\rangle_L + \beta|1\rangle_L \\ &= \alpha|000\rangle + \beta|111\rangle = |\psi\rangle_L. \end{aligned} \quad (19)$$

Fig. 2 illustrates the quantum circuit required to encode a single logical qubit via the initialization of two ancilla qubits and two CNOT gates. The reason why this

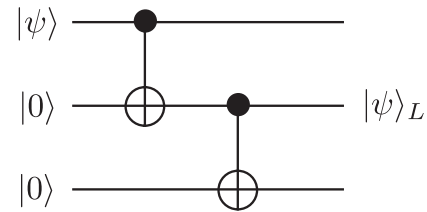


FIG. 2 Quantum Circuit to prepare the  $|0\rangle_L$  state for the 3-qubit code where an arbitrary single qubit state,  $|\psi\rangle$  is coupled to two freshly initialized ancilla qubits via CNOT gates to prepare  $|\psi\rangle_L$ .

code is able to correct for a single bit flip error is the binary distance between the two codeword states. Notice that three individual bit flips are required to take  $|0\rangle_L \leftrightarrow |1\rangle_L$ , hence if we assume  $|\psi\rangle = |0\rangle_L$ , a single bit

flip on any qubit leaves the final state closer to  $|0\rangle_L$  than  $|1\rangle_L$ . The distance between two codeword states,  $d$ , defines the number of errors that can be corrected,  $t$ , as,  $t = \lfloor (d-1)/2 \rfloor$ . In this case,  $d = 3$ , hence  $t = 1$ .

How are we able to correct errors using this code without directly measuring or obtaining information about the logical state? Two additional ancilla qubits are introduced, which are used to extract *syndrome* information (information regarding possible errors) from the data block without discriminating the exact state of any qubit, Fig. 3 illustrates. For the sake of simplicity we assume that all gate operations are perfect and the only place where the qubits are susceptible to error is the region between encoding and correction. We will return to this issue in section X when we discuss Fault-tolerance. We also assume that at most, a single, complete bit flip error occurs on one of the three data qubits. Correction proceeds by introducing two ancilla qubits and performing a sequence of CNOT gates, which checks the parity of the three qubits. Table I summarizes the state of the whole system, for each possible error, just prior to measurement.

Error Location	Final State, $ \text{data}\rangle  \text{ancilla}\rangle$
No Error	$\alpha  000\rangle  00\rangle + \beta  111\rangle  00\rangle$
Qubit 1	$\alpha  100\rangle  11\rangle + \beta  011\rangle  11\rangle$
Qubit 2	$\alpha  010\rangle  10\rangle + \beta  101\rangle  10\rangle$
Qubit 3	$\alpha  001\rangle  01\rangle + \beta  110\rangle  01\rangle$

TABLE I Final state of the five qubit system prior to the syndrome measurement for no error or a single  $X$  error on one of the qubits. The last two qubits represent the state of the ancilla. Note that each possible error will result in a unique measurement result (syndrome) of the ancilla qubits. This allows for a  $X$  correction gate to be applied to the data block which is classically controlled from the syndrome result. At no point during correction do we learn anything about  $\alpha$  or  $\beta$ .

For each possible situation, either no error or a single bit-flip error, the ancilla qubits are flipped to a unique state based on the parity of the data block. These qubits are then measured to obtain the classical *syndrome* result. The result of the measurement will then dictate if an  $X$  correction gate needs to be applied to a specific qubit, i.e.

---

Ancilla Measurement:	$ 00\rangle$ ,	Collapsed State:	$\alpha  000\rangle + \beta  111\rangle$	$\therefore$ Clean State
Ancilla Measurement:	$ 01\rangle$ ,	Collapsed State:	$\alpha  001\rangle + \beta  110\rangle$	$\therefore$ Bit Flip on Qubit 3
Ancilla Measurement:	$ 10\rangle$ ,	Collapsed State:	$\alpha  010\rangle + \beta  101\rangle$	$\therefore$ Bit Flip on Qubit 2
Ancilla Measurement:	$ 11\rangle$ ,	Collapsed State:	$\alpha  100\rangle + \beta  011\rangle$	$\therefore$ Bit Flip on Qubit 1

---

Provided that only a single error has occurred, the data block is restored. Notice that at no point during correction do we gain any information regarding the co-efficients  $\alpha$  and  $\beta$ , hence the computational wavefunction will remain intact during correction.

This code will only work if a maximum of one error occurs. If two  $X$  errors occur, then by tracking the circuit through you will see that the syndrome result becomes ambiguous. For example, if an  $X$  error occurs on both

qubits one and two, then the syndrome result will be  $|01\rangle$ . This will cause us to mis-correct by applying an  $X$  gate to qubit 3. Therefore, two errors will induce a logical bit flip and causes the code to fail, as expected.

To be absolutely clear on how QEC acts to restore the system and protect against errors. Let us now consider a different and more physically realistic error mapping. We will assume that the errors acting on the qubits are coherent rotations of the form  $U = \exp(i\epsilon\sigma_x)$  on each

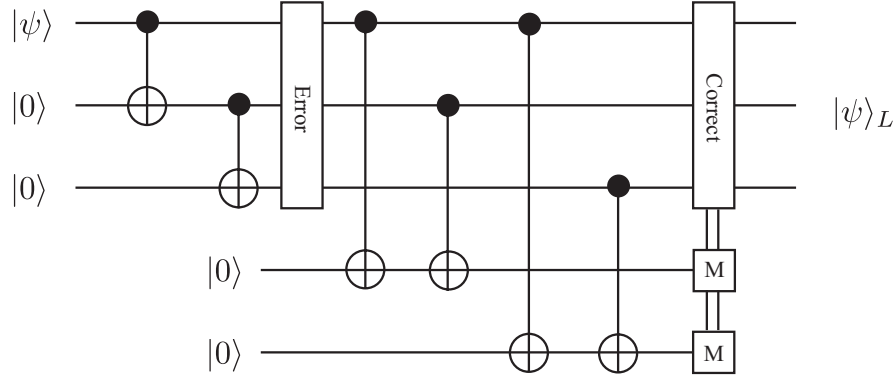


FIG. 3 Circuit required to encode and correct for a single  $X$ -error. We assume that after encoding a single bit-flip occurs on one of the three qubits (or no error occurs). Two initialized ancilla are then coupled to the data block which only checks the parity between qubits. These ancilla are then measured, with the measurement result indicating where (or if) an error has occurred, without directly measuring any of the data qubits. Using this *syndrome* information, the error can be corrected with a classically controlled  $X$  gate.

qubit, with  $\epsilon \ll 1$ . We choose coherent rotations so that we can remain in the state vector representation. This is not a necessary requirement, however more general incoherent mappings would require us to move to density matrices.

We assume that each qubit experiences the same error, hence the error operator acting on the state is,

$$\begin{aligned}
 |\psi\rangle_E &= E |\psi\rangle_L, \\
 E &= U^{\otimes 3} = (\cos(\epsilon)I + i\sin(\epsilon)\sigma_x)^{\otimes 3} \\
 &= c_0 III + c_1(\sigma_x \sigma_I \sigma_I + \sigma_I \sigma_x \sigma_I + \sigma_I \sigma_I \sigma_x) \\
 &\quad + c_2(\sigma_x \sigma_x \sigma_I + \sigma_I \sigma_x \sigma_x + \sigma_x \sigma_I \sigma_x) \\
 &\quad + c_3 \sigma_x \sigma_x \sigma_x.
 \end{aligned} \tag{21}$$

where,

$$\begin{aligned}
 c_0 &= \cos^3(\epsilon), \\
 c_1 &= i \cos^2(\epsilon) \sin(\epsilon) \\
 c_2 &= -\cos(\epsilon) \sin^2(\epsilon) \\
 c_3 &= -i \sin^3(\epsilon).
 \end{aligned} \tag{22}$$

Now let's examine the transformation that occurs when we run the error correction circuit in Fig. 3, which we denote via the unitary transformation,  $U_{QEC}$ , over *both* the data and ancilla qubits,

$$\begin{aligned}
 U_{QEC} E |\psi\rangle_L |00\rangle &= c_0 |\psi\rangle_L |00\rangle + c_1(\sigma_x \sigma_I \sigma_I |\psi\rangle_L |11\rangle + \sigma_I \sigma_x \sigma_I |\psi\rangle_L |10\rangle + \sigma_x \sigma_I \sigma_I |\psi\rangle_L |01\rangle) \\
 &\quad + c_2(\sigma_x \sigma_x \sigma_I |\psi\rangle_L |10\rangle + \sigma_I \sigma_x \sigma_x |\psi\rangle_L |11\rangle + X I X |\psi\rangle_L |01\rangle) + c_3 \sigma_x \sigma_x \sigma_x |\psi\rangle_L |00\rangle
 \end{aligned} \tag{23}$$

Once again, the ancilla block is measured and the appropriate correction operator is applied, yielding the results

(up to renormalization),

$$\begin{aligned}
 \text{Ancilla Measurement: } |00\rangle, & \quad \text{Collapsed State (with correction): } c_0 |\psi\rangle_L + c_3 \sigma_x \sigma_x \sigma_x |\psi\rangle_L \\
 \text{Ancilla Measurement: } |01\rangle, & \quad \text{Collapsed State (with correction): } c_1 |\psi\rangle_L + c_2 \sigma_x \sigma_x \sigma_x |\psi\rangle_L \\
 \text{Ancilla Measurement: } |10\rangle, & \quad \text{Collapsed State (with correction): } c_1 |\psi\rangle_L + c_2 \sigma_x \sigma_x \sigma_x |\psi\rangle_L \\
 \text{Ancilla Measurement: } |11\rangle, & \quad \text{Collapsed State (with correction): } c_1 |\psi\rangle_L + c_2 \sigma_x \sigma_x \sigma_x |\psi\rangle_L
 \end{aligned} \tag{24}$$

In each case, after correction (based on the syndrome result), we are left with approximately the same state. A



superposition of a “clean state” with the logically flipped state,  $\sigma_x \sigma_x \sigma_x |\psi\rangle$ . The important thing to notice is the amplitudes related to the terms in the superposition. If we consider the unitary  $U$  acting on a single, unencoded qubit, the rotation takes,

$$U|\psi\rangle = \cos(\epsilon)|\psi\rangle + i\sin(\epsilon)\sigma_x|\psi\rangle, \quad (25)$$

Consequently, the fidelity of the single qubit state is,

$$F_{\text{unencoded}} = |\langle\psi|U|\psi\rangle|^2 = \cos^2 \epsilon \approx 1 - \epsilon^2 \quad (26)$$

In contrast, the fidelity of the encoded qubit state after a cycle of error correction is,

$$F_{\text{no detection}} = \frac{|c_0|^2}{|c_0|^2 + |c_3|^2} = \frac{\cos^6(\epsilon)}{\cos^6(\epsilon) + \sin^6(\epsilon)} \quad (27)$$

$$\approx 1 - \epsilon^6,$$

with probability  $1 - 3\epsilon^2 + O(\epsilon^4)$  and

$$F_{\text{error detected}} = \frac{|c_1|^2}{|c_1|^2 + |c_2|^2} \quad (28)$$

$$= \frac{\cos^4(\epsilon)\sin^2(\epsilon)}{\cos^4(\epsilon)\sin^2(\epsilon) + \sin^4(\epsilon)\cos^2(\epsilon)}$$

$$\approx 1 - \epsilon^2.$$

with probability  $3\epsilon^2 + O(\epsilon^4)$ . This is the crux of how QEC suppresses errors at the logical level. During a round of error correction, if no error is detected (which if the error rate is small, occurs with high probability), the error on the resulting state is suppressed from  $O(\epsilon^2)$  to  $O(\epsilon^6)$ , while if a single error is detected, the fidelity of the resulting state remains the same.

This is expected, as the 3-qubit code is a single error correcting code. If one error has already been corrected then the failure rate of the logical system is conditional on experiencing one further error (which will be proportional to  $\epsilon^2$ ). As  $\epsilon \ll 1$  the majority of correction cycles will detect no error and the fidelity of the resulting encoded state is higher than when unencoded. Note, that as  $\epsilon^2 \rightarrow 1/3$  the benefit of the code disappears as every correction cycle detects an error and the resulting fidelity is no better than an unencoded qubit

It should be stressed that **no error correction scheme will, in general, restore a corrupted state to a perfectly clean code-state**. The resulting state will contain a superposition of a clean state and corrupted states, the point is that the fidelity of the corrupted states, at the logical level, is greater than the corresponding fidelity for unencoded qubits. Consequently the probability of measuring the correct result at the end of a specific algorithm increases when the system is encoded.

This example shows the basic principles of error correction. As mentioned earlier, the 3-qubit code does not represent a full quantum code and the error model that we considered neglected imperfect gates and the possibility of errors occurring during state preparation and/or

correction. In the coming sections we will briefly take a look at several full quantum codes, both used for quantum memory and computation and we will introduce the concept of full QEC using stabilizer codes. This will then lead to a description of full fault-tolerant quantum error correction.

## V. THE NINE QUBIT CODE: THE FIRST FULL QUANTUM CODE

The nine qubit error correcting code was first developed by Shor (Sho95) in 1995 and is based largely on the 3-qubit repetition code. The Shor code is a degenerate single error correcting code able to correct a logical qubit from one discrete bit flip, one discrete phase flip or one of each on any of the nine physical qubits and is therefore sufficient to correct for any continuous linear combination of errors on a single qubit. The two basis states for the code are,

$$|0\rangle_L = \frac{1}{\sqrt{8}}(|000\rangle + |111\rangle)(|000\rangle + |111\rangle)(|000\rangle + |111\rangle)$$

$$|1\rangle_L = \frac{1}{\sqrt{8}}(|000\rangle - |111\rangle)(|000\rangle - |111\rangle)(|000\rangle - |111\rangle) \quad (29)$$

and the circuit to perform the encoding is shown in Fig. 4. Correction for  $X$  errors, for each block of three qubits

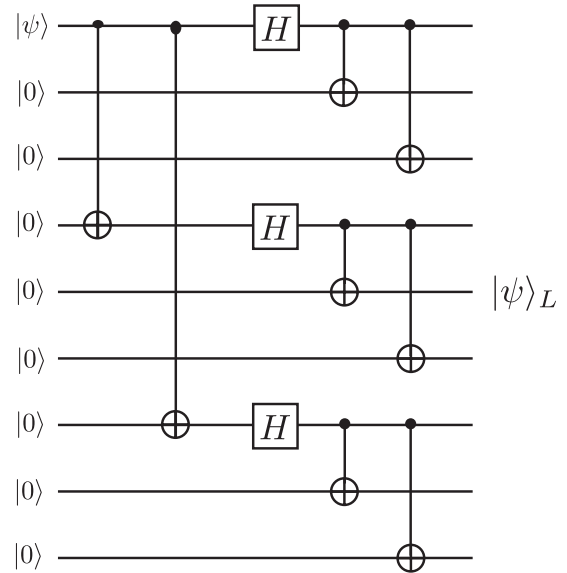


FIG. 4 Circuit required to encode a single qubit with Shor’s nine qubit code.

encoded to  $(|000\rangle \pm |111\rangle)/\sqrt{2}$  is identical to the three qubit code shown earlier. By performing the correction circuit shown in Fig. 3 for each block of three qubits, single  $\sigma_x \equiv X$  errors can be detected and corrected. Phase errors ( $\sigma_z \equiv Z$ ) are corrected by examining the sign differences between the three blocks. The circuit shown

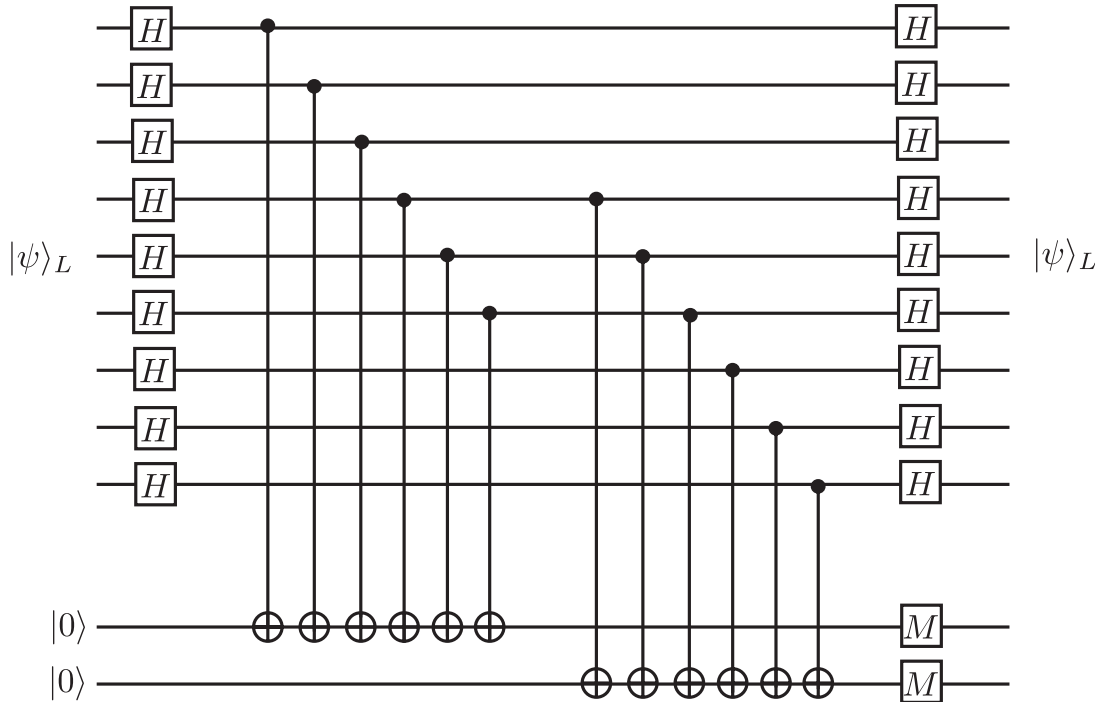


FIG. 5 Circuit required to encode a single qubit with Shor's nine qubit code.

in Fig. 5 achieves this. The first set of six CNOT gates compares the sign of blocks one and two of the code state and the second set of CNOT gates compares the sign for blocks two and three. Note that a phase flip on *any* one qubit in a block of three has the same effect, this is why the 9-qubit code is referred to as a degenerate code. In other error correcting codes, such as the 5- or 7-qubit codes (Ste96a; LMPZ96), there is a one-to-one mapping between correctable errors and unique states, in degenerate codes such as this, the mapping is not unique. Hence provided we know in which block the error occurs it does not matter which qubit we apply the correction operator to.

As the 9-qubit code can correct for single  $X$  errors in any one block of three and a single phase error on any of the nine qubits, this code is a full quantum error correcting code (we will detail in section IX why phase and bit correction is sufficient for the correction of arbitrary qubit errors). Even if a bit *and* phase error occurs on the same qubit, the  $X$  correction circuit will detect and correct for bit flips while the  $Z$  correction circuit will detect and correct for phase flips. As mentioned, the  $X$  error correction does have the ability to correct for up to three individual bit flips (provided each bit flip occurs in a different block of three). However, in general the 9-qubit code is only a single error correcting code as it cannot handle multiple errors if they occur in certain locations.

The 9-qubit code is in fact a member of a broader class of error correcting codes known as Bacon-Shor or subsystem codes (Bac06). Subsystem codes have the property

that certain subgroups of error operators do not corrupt the logical space. This can be seen by considering phase errors that occur in pairs for any block of three. For example, a phase flip on qubits one, two, four and five will leave both logical states unchanged. Subsystem codes are very nice codes from an architectural point of view. Error correction circuits and gates are generally simpler than for non-subsystem codes, allowing for circuit structures more amenable to the physical restrictions of a computer architecture (AC07). Additionally as subsystem codes that can correct for a larger number of errors have a similar structure, we are able to perform dynamical switching between codes, in a fault-tolerant manner, which allows us to adapt the error protection in the computer to be changed depending on the noise present at a physical level (SEDH07). We will return and revisit subsystem codes later in section XIV.A

## VI. QUANTUM ERROR DETECTION

So far we have focused on the ability to not only detect errors, but also to correct them. Another approach is to not enforce the correction requirement. Post-selected quantum computation, developed by Knill (Kni05) demonstrated that large scale quantum computing could be achieved with much higher noise rates when error detection is employed instead of more costly correction protocols. The basic idea in post-selected schemes is to encode the computer with error detecting circuits and if errors are detected, the relevant subroutine of the quantum

algorithm is reset and run again, instead of performing active correction. One of the downside to these types of schemes is that although they lead to large tolerable error rates, the resource requirements are unrealistically high.

The simplest error detecting circuit is the 4-qubit code (GBP97). This encodes two logical qubits into four physical qubits with the ability to detect a single error on either of the two logical qubits. The four basis states for the code are,

$$\begin{aligned} |00\rangle &= \frac{1}{\sqrt{2}}(|0000\rangle + |1111\rangle), \\ |01\rangle &= \frac{1}{\sqrt{2}}(|1100\rangle + |0011\rangle), \\ |10\rangle &= \frac{1}{\sqrt{2}}(|1010\rangle + |0101\rangle), \\ |11\rangle &= \frac{1}{\sqrt{2}}(|0110\rangle + |1001\rangle). \end{aligned} \quad (30)$$

Fig. 6 illustrates the error detection circuit that can be utilized to detect a single bit and/or phase flip on one of these encoded qubits. If a single bit and/or phase flip occurs on one of the four qubits then the ancilla qubits will be measured in the  $|1\rangle$  state. For example, let us consider the cases when a single bit flip occurs on one of each of the four qubits. The state of the system, just prior to the measurement of the ancilla is in table. II. Regardless of

Error Location	Final State, $ \text{data}\rangle  \text{ancilla}\rangle$
No Error	$ \psi\rangle_L  00\rangle$
Qubit 1	$X_1  \psi\rangle_L  10\rangle$
Qubit 2	$X_2  \psi\rangle_L  10\rangle$
Qubit 3	$X_3  \psi\rangle_L  10\rangle$
Qubit 4	$X_4  \psi\rangle_L  10\rangle$

TABLE II Qubit and ancilla state, just prior to measurement for the 4-qubit error detection code when a single bit-flip has occurred on at most one of the four qubits.

the location of the bit flip, the ancilla system is measured in the state  $|10\rangle$ . Similarly if one considers a single phase error on any of the four qubits the ancilla measurement will return  $|01\rangle$ . In both cases no information is obtained regarding *where* the error has occurred, hence it is not possible to correct the state. Instead the subroutine can be reset and re-run.

## VII. STABILIZER FORMALISM

So far we have presented error correcting codes from the perspective of their state representations and their preparation and correction circuits. This is a rather inefficient method for describing the codes as the state representations and circuits clearly differ from code to code. The majority of error correcting codes that are used within the literature are members of a class known

as stabilizer codes. Stabilizer codes are very useful to work with. The general formalism applies broadly and there exists general rules to construct preparation circuits, correction circuits and fault-tolerant logical gate operations once the stabilizer structure of the code is specified.

The stabilizer formalism which was first introduced by Daniel Gottesman (Got97) uses essentially the Heisenberg representation for quantum mechanics which describes quantum states in terms of operators rather than the basis states themselves. An arbitrary state  $|\psi\rangle$  is defined to be stabilized by some operator,  $K$ , if it is a  $+1$  eigenstate of  $K$ , i.e.

$$K |\psi\rangle = |\psi\rangle. \quad (31)$$

For example, the single qubit state  $|0\rangle$  is stabilized by the operator  $K = \sigma_z$ , i.e.

$$\sigma_z |0\rangle = |0\rangle \quad (32)$$

Defining multi-qubit states with respect to this formalism relies on the group structure of multi-qubit operators.

Within the group of all possible, single qubit operators, there exists a subgroup, denoted the Pauli group,  $\mathcal{P}$ , which contains the following elements,

$$\mathcal{P} = \{\pm\sigma_I, \pm i\sigma_I, \pm\sigma_x, \pm i\sigma_x, \pm\sigma_y, \pm i\sigma_y, \pm\sigma_z, \pm i\sigma_z\}. \quad (33)$$

It is easy to check that these matrices form a group under multiplication through the commutation and anti-commutation rules for the Pauli set,  $\{\sigma_i\} = \{\sigma_x, \sigma_y, \sigma_z\}$ ,

$$[\sigma_i, \sigma_j] = 2i\epsilon_{ijk}\sigma_k, \quad \{\sigma_i, \sigma_j\} = 2\delta_{ij}, \quad (34)$$

where,

$$\epsilon_{ijk} = \begin{cases} +1 & \text{for } (i, j, k) \in \{(1, 2, 3), (2, 3, 1), (3, 1, 2)\} \\ -1 & \text{for } (i, j, k) \in \{(1, 3, 2), (3, 2, 1), (2, 1, 3)\} \\ 0 & \text{for } i = j, j = k, \text{ or } k = i \end{cases} \quad (35)$$

and

$$\delta_{ij} = \begin{cases} 1 & \text{for } i = j \\ 0 & \text{for } i \neq j. \end{cases} \quad (36)$$

The Pauli group extends over  $N$ -qubits by simply taking the  $N$  fold tensor product of  $\mathcal{P}$ , i.e.

$$\begin{aligned} \mathcal{P}_N &= \mathcal{P}^{\otimes N} \\ &= \{\pm\sigma_I, \pm i\sigma_I, \pm\sigma_x, \pm i\sigma_x, \pm\sigma_y, \pm i\sigma_y, \pm\sigma_z, \pm i\sigma_z\}^{\otimes N}. \end{aligned} \quad (37)$$

An  $N$ -qubit stabilizer state,  $|\psi\rangle_N$  is then defined via an  $N$ -element Abelian subgroup,  $\mathcal{G}$ , of the  $N$ -qubit Pauli group, in which  $|\psi\rangle_N$  is a  $+1$  eigenstate of each element,

$$\begin{aligned} \mathcal{G} &= \\ &\{ G_i \mid G_i |\psi\rangle = |\psi\rangle, [G_i, G_j] = 0 \forall (i, j) \} \subset \mathcal{P}_N. \end{aligned} \quad (38)$$

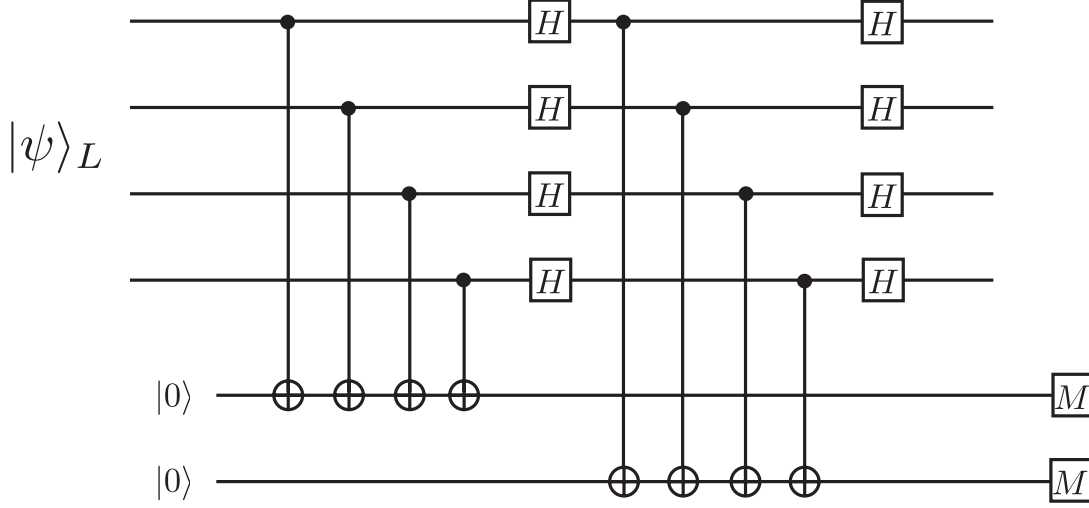


FIG. 6 Circuit required detect errors in the 4-qubit error detection code. If both ancilla measurements return  $|0\rangle$ , then the code state is error free. If either measurement returns  $|1\rangle$ , an error has occurred. Unlike the 9-qubit code, the detection of an error does not give sufficient information to correct the state.

Given this definition, the state  $|\psi\rangle_N$  can be equivalently defined either through the state vector representation *or* by specifying the stabilizer set,  $\mathcal{G}$ .

Many extremely useful multi-qubit states are stabilizer states, including two-qubit Bell states, Greenberger-Horne-Zeilinger (GHZ) states (GHZ89; GHSZ90), Cluster states (BR01; RB01) and codeword states for QEC. As an example, consider a three qubit GHZ state, defined as,

$$|\text{GHZ}\rangle_3 = \frac{|000\rangle + |111\rangle}{\sqrt{2}}. \quad (39)$$

This state can be expressed via any three linearly independent elements of the  $|\text{GHZ}\rangle_3$  stabilizer group for example,

$$\begin{aligned} G_1 &= \sigma_x \otimes \sigma_x \otimes \sigma_x \equiv XXX, \\ G_2 &= \sigma_z \otimes \sigma_z \otimes \sigma_I \equiv ZZI, \\ G_3 &= \sigma_I \otimes \sigma_z \otimes \sigma_z \equiv IZZ. \end{aligned} \quad (40)$$

where the right-hand side of each equation is the shorthand representation of stabilizers. Note that these three operators form an Abelian group [Eq. 38] as,

$$\begin{aligned} |\psi\rangle &= G_i G_j |\psi\rangle = G_j G_i |\psi\rangle \\ &= |\psi\rangle - |\psi\rangle = 0, \quad \forall \quad [i, j, |\psi\rangle]. \end{aligned} \quad (41)$$

Similarly, the four orthogonal Bell states,

$$\begin{aligned} |\Phi^\pm\rangle &= \frac{|00\rangle \pm |11\rangle}{\sqrt{2}}, \\ |\Psi^\pm\rangle &= \frac{|01\rangle \pm |10\rangle}{\sqrt{2}}, \end{aligned} \quad (42)$$

are stabilized by the operators,  $G_1 = (-1)^a XX$ , and  $G_2 = (-1)^b ZZ$ . Where  $[a, b] \in \{0, 1\}$  and each of the four Bell states correspond to the four unique pairs,  $\{\Phi^+, \Psi^+, \Phi^-, \Psi^-\} = \{[0, 0], [0, 1], [1, 0], [1, 1]\}$ .

### VIII. QEC WITH STABILIZER CODES

The use of the stabilizer formalism to describe quantum error correction codes is extremely useful since it allows for easy synthesis of correction circuits and also clearly shows how logical operations can be performed directly on encoded data. As an introduction we will focus on arguably the most well known quantum code, the 7-qubit Steane code, first proposed in 1996 (Ste96a).

The 7-qubit code represents a full quantum code that encodes seven physical qubits into one logical qubit, with the ability to correct for a single  $X$  and/or  $Z$  error. The  $|0\rangle_L$  and  $|1\rangle_L$  basis states are defined as,

$$\begin{aligned} |0\rangle_L &= \frac{1}{\sqrt{8}}(|0000000\rangle + |1010101\rangle + |0110011\rangle + |1100110\rangle + |0001111\rangle + |1011010\rangle + |0111100\rangle + |1101001\rangle), \\ |1\rangle_L &= \frac{1}{\sqrt{8}}(|1111111\rangle + |0101010\rangle + |1001100\rangle + |0011001\rangle + |1110000\rangle + |0100101\rangle + |1000011\rangle + |0010110\rangle). \end{aligned} \quad (43)$$

The stabilizer set for the 7-qubit code is fully specified by the six operators,

$$\begin{aligned} K^1 &= IIIXXXX, & K^2 &= XIXIXIX, \\ K^3 &= IXXIIXX, & K^4 &= IIIZZZZ \\ K^5 &= ZIZIZIZ, & K^6 &= IZZIIZZ. \end{aligned} \quad (44)$$

As the 7-qubit codeword states are specified by only six stabilizers, the code contains two basis states, which are the logical states. With a final operator,  $K^7 = ZZZZZZZ = Z^{\otimes 7}$  fixing the state to one of the codewords,  $K^7|0\rangle_L = |0\rangle_L$  and  $K^7|1\rangle_L = -|1\rangle_L$ . The 7-qubit code is defined as a  $[[n, k, d]] = [[7, 1, 3]]$  quantum code, where  $n = 7$  physical qubits encode  $k = 1$  logical qubit with a distance between basis states  $d = 3$ , correcting  $t = (d-1)/2 = 1$  error. Notice that the stabilizer set separates into  $X$  and  $Z$  sectors which defines the code as a Calderbank-Shor-Steane (CSS) code. CSS codes are extremely useful since they allow for straightforward logical gate operations to be applied directly to the encoded data [Section XI] and are reasonably easy to derive from classical codes.

Although the 7-qubit code is the most well known Stabilizer code, there are other stabilizer codes which encode multiple logical qubits and correct for more errors (Got97). The downside to these larger codes is that they require more physical qubits and more complicated error correction circuits. Tables III and IV shows the stabilizer structure of two other well known codes, the 9-qubit code (Sho95) which we have examined and the 5-qubit code (LMPZ96) which represents the smallest possible quantum code that corrects for a single error.

$K^1$	Z	Z	I	I	I	I	I	I	I
$K^2$	Z	I	Z	I	I	I	I	I	I
$K^3$	I	I	I	Z	Z	I	I	I	I
$K^4$	I	I	I	Z	I	Z	I	I	I
$K^5$	I	I	I	I	I	I	Z	Z	I
$K^6$	I	I	I	I	I	I	Z	I	Z
$K^7$	X	X	X	X	X	X	I	I	I
$K^8$	X	X	X	I	I	I	X	X	X

TABLE III The eight Stabilizers for the 9-qubit Shor code, encoding nine physical qubits into one logical qubit to correct for a single  $X$  and/or  $Z$  error.

### A. State Preparation

Using the stabilizer structure for QEC codes, the logical state preparation and error correcting procedure is straightforward. Recall that the codeword states are defined as  $+1$  eigenstates of the stabilizer set. In order to prepare a logical state from some arbitrary input, we need to forcibly project qubits into eigenstates of these operators.

$K^1$	X	Z	Z	X	I
$K^2$	I	X	Z	Z	X
$K^3$	X	I	X	Z	Z
$K^4$	Z	X	I	X	Z

TABLE IV The Four Stabilizers for the  $[[5,1,3]]$  quantum code, encoding five physical qubits into one logical qubit to correct for a single  $X$  and/or  $Z$  error. Unlike the 7- and 9-qubit codes, the  $[[5,1,3]]$  code is a non-CSS code, since the stabilizer set does not separate into  $X$  and  $Z$  sectors.

Consider the circuit shown in Fig. 7. For some arbitrary

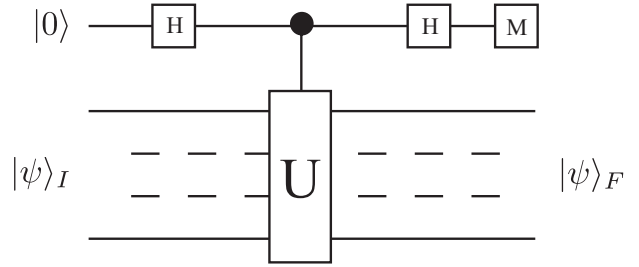


FIG. 7 Quantum Circuit required to project an arbitrary state,  $|\psi\rangle_I$  into a  $\pm 1$  eigenstate of the Hermitian operator,  $U = U^\dagger$ . The measurement result of the ancilla determines which eigenstate  $|\psi\rangle_I$  is projected to.

trary input state,  $|\psi\rangle_I$ , an ancilla which is initialized in the  $|0\rangle$  state is used as a control qubit for a Hermitian operation ( $U^\dagger = U$ ) on  $|\psi\rangle_I$ . After the second Hadamard gate is performed, the state of the system is,

$$|\psi\rangle_F = \frac{1}{2}(|\psi\rangle_I + U|\psi\rangle_I)|0\rangle + \frac{1}{2}(|\psi\rangle_I - U|\psi\rangle_I)|1\rangle. \quad (45)$$

The ancilla qubit is then measured in the computational basis. If the result is  $|0\rangle$ , the input state is projected to (neglecting normalization),

$$|\psi\rangle_F = |\psi\rangle_I + U|\psi\rangle_I. \quad (46)$$

Since  $U$  is Hermitian,  $U|\psi\rangle_F = |\psi\rangle_F$ , hence  $|\psi\rangle_F$  is a  $+1$  eigenstate of  $U$ . If the ancilla is measured to be  $|1\rangle$ , then the input is projected to the state,

$$|\psi\rangle_F = |\psi\rangle_I - U|\psi\rangle_I, \quad (47)$$

which is the  $-1$  eigenstate of  $U$ . Therefore, provided  $U$  is Hermitian, the general circuit of Fig. 7 will project an arbitrary input state to a  $\pm 1$  eigenstate of  $U$ . This procedure is well known and is referred to as either a “parity” or “operator” measurement (NC00).

From this construction it should be clear how QEC state preparation proceeds. Taking the  $[[7,1,3]]$  code as an example, 7-qubits are first initialized in the state  $|0\rangle^{\otimes 7}$ , after which the circuit shown in Fig. 7 is applied three times with  $U = (K^1, K^2, K^3)$ , projecting the input

state into a simultaneous  $\pm 1$  eigenstate of each  $X$  stabilizer describing the  $[[7, 1, 3]]$  code. The result of each operator measurement is then used to classically control a single qubit  $Z$  gate which is applied to one of the seven qubits at the end of the preparation. This single  $Z$  gate converts any  $-1$  projected eigenstates into  $+1$  eigenstates. Notice that the final three stabilizers do not need to be measured due to the input state,  $|0\rangle^{\otimes 7}$ , already being a  $+1$  eigenstate of  $(K^4, K^5, K^6)$ . Fig. 8 illustrates the final circuit, where instead of one ancilla, three are utilized to speed up the state preparation by performing each operator measurement in parallel.

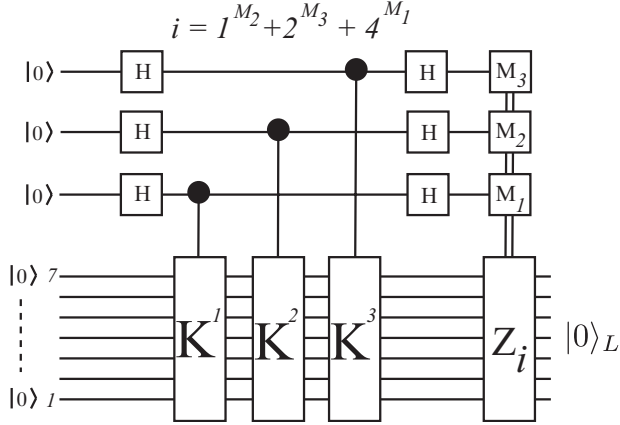


FIG. 8 Quantum circuit to prepare the  $[[7, 1, 3]]$  logical  $|0\rangle$  state. The input state  $|0\rangle^{\otimes 7}$  is projected into an eigenstate of each of the  $X$  stabilizers shown in Eq. 44. After each ancilla measurement the classical results are used to apply a single qubit  $Z$  gate to qubit  $i = 1^{M_2} + 2^{M_3} + 4^{M_1}$  which converts the state from a  $-1$  eigenstates of  $(K^1, K^2, K^3)$  to  $+1$  eigenstates.

As a quick aside, let us detail exactly how the relevant logical basis states can be derived from the stabilizer structure of the code by utilizing the preparation circuit illustrated above. Instead of the 7-qubit code, we will use the stabilizer set shown in Table IV to calculate the  $|0\rangle_L$  state for the 5-qubit code. The four code stabilizers are given by,

$$\begin{aligned} K^1 &= XZZXI, & K^2 &= IXZZX, \\ K^3 &= XIXZZ, & K^4 &= ZXIXZ. \end{aligned} \quad (48)$$

As with the 7-qubit code, projecting an arbitrary state into a  $+1$  eigenstate of these operators define the two, logical basis states  $|0\rangle_L$  and  $|1\rangle_L$ , with the operator  $\bar{Z} = ZZZZZ$ , fixing the state to either  $|0\rangle_L$  or  $|1\rangle_L$ . Therefore, calculating  $|0\rangle_L$  from some initial un-encoded state requires us to project the initial state into a  $+1$  eigenstate of these operators. If we take the initial, un-encoded state as  $|00000\rangle$ , then it already is a  $+1$  eigenstate of  $\bar{Z}$ . Therefore, to find  $|0\rangle_L$  we simply calculate,

$$|0\rangle_L = \prod_{i=1}^4 (I^{\otimes 5} + K^i) |00000\rangle, \quad (49)$$

up to normalization. Expanding out this product, we find,

$$\begin{aligned} |0\rangle_L = \frac{1}{4} (&|00000\rangle + |01010\rangle + |10100\rangle - |11110\rangle + \\ &|01001\rangle - |00011\rangle - |11101\rangle - |10111\rangle + \\ &|10010\rangle - |11000\rangle - |00110\rangle - |01100\rangle - \\ &|11011\rangle - |10001\rangle - |01111\rangle + |00101\rangle). \end{aligned} \quad (50)$$

Note, that the above state vector does not match up with those given in (LMPZ96). However, these vectors are equivalent up to local rotations on each qubit. Therefore, matching up the original state requires locally perturbing the stabilizer set to reflect these rotations.

## B. Error Correction

Error correction using stabilizer codes is a straightforward extension of state preparation. Consider an arbitrary single qubit state that has been encoded,

$$\alpha |0\rangle + \beta |1\rangle \rightarrow \alpha |0\rangle_L + \beta |1\rangle_L = |\psi\rangle_L. \quad (51)$$

Now assume that an error occurs on one (or multiple) qubits which is described via the operator  $E$ , where  $E$  is a combination of  $X$  and/or  $Z$  errors over the  $N$  physical qubits of the logical state. By definition of stabilizer codes,  $K^i |\psi\rangle_L = |\psi\rangle_L$ ,  $i \in [1, \dots, N - k]$ , for a code encoding  $k$  logical qubits. Hence the erred state,  $E |\psi\rangle_L$ , satisfies,

$$K^i E |\psi\rangle_L = (-1)^m E K^i |\psi\rangle_L = (-1)^m E |\psi\rangle_L. \quad (52)$$

where  $m$  is defined as,  $m = 0$ , if  $[E, K^i] = 0$  and  $m = 1$ , if  $\{E, K^i\} = 0$ . Therefore, if the error operator commutes with the stabilizer, the state remains a  $+1$  eigenstate of  $K^i$ , if the error operator anti-commutes with the stabilizer then the logical state is flips to now be a  $-1$  eigenstate of  $K^i$ .

Hence the general procedure for error correction is identical to state preparation. Each of the code stabilizers are sequentially measured. Since a error free state is already a  $+1$  eigenstate of all the stabilizers, any error which anti-commutes with a stabilizer will flip the eigenstate and consequently the parity measurement will return a result of  $|1\rangle$ .

Taking the  $[[7, 1, 3]]$  code as an example, you can see that if the error operator is  $E = X_i$ , where  $i = (1, \dots, 7)$ , representing a bit-flip on any *one* of the 7 physical qubits, then regardless of the location,  $E$  will anti-commute with a unique combination of  $(K^4, K^5, K^6)$ . Hence the classical results of measuring these three operators will indicate if and where a single  $X$  error has occurred. Similarly, if  $E = Z_i$ , then the error operator will anti-commute with a unique combination of,  $(K^1, K^2, K^3)$ . Consequently, the first three stabilizers for the  $[[7, 1, 3]]$  code correspond to  $Z$  sector correction while the second three stabilizers correspond to  $X$  sector correction. Note, that correction

for Pauli  $Y$  errors are also taken care of by correcting in the  $X$  and  $Z$  sector since a  $Y$  error on a single qubit is equivalent to both an  $X$  and  $Z$  error on the same qubit, i.e.  $Y = iXZ$ .

Fig. 9 illustrates the circuit for full error correction with the  $[[7, 1, 3]]$  code. As you can see it is simply an extension of the preparation circuit [Fig. 8] where all six stabilizers are measured across the data block. Even though we have specifically used the  $[[7, 1, 3]]$  code as an example, the procedure for error correction and state preparation is identical for all stabilizer codes allowing for full correction for both bit and phase errors without obtaining any information regarding the state of the logical qubit.

## IX. DIGITIZATION OF QUANTUM ERRORS

Up until now we have remained fairly abstract regarding the analysis of quantum errors. Specifically, we have examined QEC from the standpoint of a discrete set of Pauli errors occurring at certain locations within a larger quantum circuit. In this section we examine how this analysis of errors relates to more realistic processes such as environmental decoherence and systematic gate errors.

Digitization of quantum noise is often assumed when people examine the stability of quantum circuit design or attempt to calculate thresholds for concatenated error correction. However, the equivalence of discrete Pauli errors to more general, continuous, noise only makes sense when we consider the stabilizer nature of the correction procedure. Recall from section VII that correction is performed by re-projecting a potentially corrupt data block into  $+1$  eigenstates of the stabilizer set. It is this process that acts to digitize quantum noise, since a general continuous mapping from a “clean” codeword state to a corrupt one will not satisfy the stabilizer conditions. we will first introduce how a coherent systematic error, caused by imperfect implementation of quantum gates, are digitized during correction, after which we will briefly discuss environmental decoherence from the standpoint of the Markovian decoherence model.

### A. Systematic gate errors

We have already shown an example of how systematic gate errors are digitized into a discrete set of Pauli operators in Sec. III. However, in that case we only considered a very restrictive type of error, namely the coherent operator  $U = \exp(i\epsilon X)$ . We can easily extend this analysis to cover all forms of systematic gate errors. Consider an  $N$  qubit unitary operation,  $U_N$ , which is valid on encoded data. Assume that  $U_N$  is applied inaccurately such that the resultant operation is actually  $U'_N$ . Given a general encoded state  $|\psi\rangle_N$ , the final state can be expressed as,

$$U'_N |\psi\rangle_L = U_E U_N |\psi\rangle_L = \sum_j \alpha_j E_j |\psi'\rangle_L, \quad (53)$$

where  $|\psi'\rangle_L = U_N |\psi\rangle_L$  is the perfectly applied  $N$  qubit gate, (i.e. the stabilizer set for  $|\psi'\rangle_L$  remains invariant under the operation  $U_N$  [see Sec. XI]). and  $U_E$  is a coherent error operator which is expanded in terms of the  $N$  qubit Pauli Group,  $E_j \in P_N$ . Now append two ancilla blocks,  $|A_0\rangle^X$  and  $|A_0\rangle^Z$ , which are all initialized and are used for  $X$  and  $Z$  sector correction, then run a full error correction cycle, which we represent by the unitary operator,  $U_{\text{QEC}}$ . It will be assumed that  $|\psi\rangle_L$  is encoded with a *hypothetical* QEC code which can correct for  $N$  errors (both  $X$  and/or  $Z$ ), hence there is a one-to-one mapping between the error operators,  $E_j$ , and the orthogonal basis states of the ancilla blocks,

$$\begin{aligned} U_{\text{QEC}} U'_N |\psi\rangle_L |A_0\rangle^X |A_0\rangle^Z \\ = U_{\text{QEC}} \sum_j \alpha_j E_j |\psi'\rangle_L |A_0\rangle^X |A_0\rangle^Z \\ = \sum_j \alpha_j E_j |\psi'\rangle_L |A_j\rangle^X |A_j\rangle^Z. \end{aligned} \quad (54)$$

The ancilla blocks are then measured, projecting the data blocks into the state  $E_j |\psi'\rangle_L$  with probability  $|\alpha_j|^2$ , after which the correction  $E_j^\dagger$  is applied based on the syndrome result. As the error operation  $E_j$  is simply an element of  $\mathcal{P}_N$ , correcting for  $X$  and  $Z$  independently is sufficient to correct for all error operators (as  $Y$  errors are corrected when a bit and phase error is detected and corrected on the same qubit).

For very small systematic inaccuracies, the expansion co-efficient,  $\alpha_0$ , which corresponds to  $E_0 = I^{\otimes N}$  will be very close to 1, with all other co-efficients small. Hence during correction there will be a very high probability that no error is detected. This is the digitization effect of quantum error correction. Since codeword states are specific eigenstates of the stabilizers, then the re-projection of the state when each stabilizer is measured forces any continuous noise operator to collapse to the discrete Pauli set, with the magnitude of the error dictating the probability that the data block is projected into discrete perturbation of a “clean” state.

### B. Environmental decoherence

A complete analysis of environmental decoherence in relation to quantum information is a lengthy topic. Instead of a detailed review, we will instead simply present a specific example to highlight how QEC relates to environmental effects.

The Lindblad formalism (Gar91; NC00; DWM03) provides an elegant method for analyzing the effect of decoherence on open quantum systems. This model does have several assumptions, most notably that the environmental bath couples weakly to the system (Born approximation) and that each qubit experiences un-correlated noise (Markovian approximation). While these assumptions are utilized for a variety of systems (BHPC03; BM03;



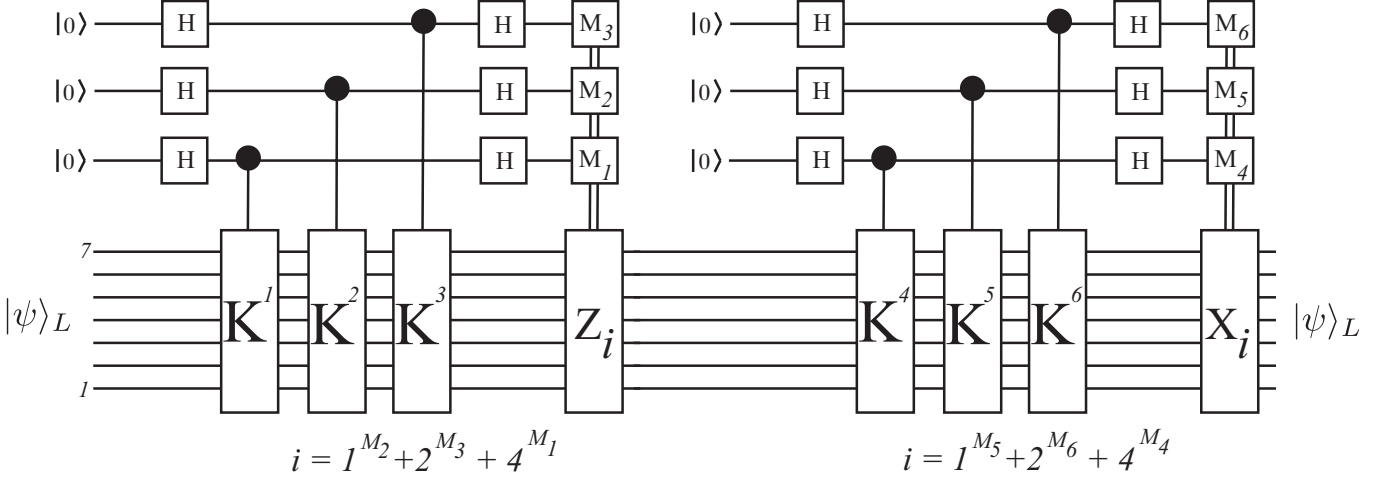


FIG. 9 Quantum circuit to correct for a single  $X$  and/or  $Z$  error using the  $[[7, 1, 3]]$  code. Each of the 6 stabilizers are measured, with the first three detecting and correcting for  $Z$  errors, while the last three detect and correct for  $X$  errors.

BKD04), it is known that they may not hold in some cases (HMCS00; MCM<sup>+</sup>05; APN<sup>+</sup>05; ALKH02). Particularly in superconducting systems where decoherence can be caused by small numbers of fluctuating charges. In this case more specific decoherence models need to be considered.

Using this formalism, the evolution of the density matrix can be written as,

$$\partial_t \rho = -\frac{i}{\hbar} [H, \rho] + \sum_k \Gamma_k \mathcal{L}[\rho]. \quad (55)$$

Where  $H$  is the Hamiltonian, representing coherent, dynamical evolution of the system and  $\mathcal{L}_k[\rho] = ([L_k, \rho L_k^\dagger] + [L_k \rho, L_k^\dagger])/2$  represents the incoherent evolution. The operators  $L_k$  are known as the Lindblad quantum jump operators and are used to model specific decoherence channels, with each operator parameterized by some rate  $\Gamma_k \geq 0$ . This differential equation is known as the quantum liouville equation or more generally, the density matrix master equation.

To link Markovian decoherence to QEC, consider a special set of decoherence channels that help to simplify the calculation, representing a single qubit undergoing dephasing, spontaneous emission and spontaneous absorption. Dephasing of a single qubit is modelled by the Lindblad operator  $L_1 = Z$  while spontaneous emission/absorption are modelled by the operators  $L_2 = |0\rangle\langle 1|$  and  $L_3 = |1\rangle\langle 0|$  respectively. For the sake of simplicity we assume that absorption/emission occur at the same rate,  $\Gamma$ . Consequently, the density matrix evolution is given by,

$$\partial_t \rho = -\frac{i}{\hbar} [H, \rho] + \Gamma_Z (Z \rho Z - \rho) + \frac{\Gamma}{2} (X \rho X + Y \rho Y - 2\rho). \quad (56)$$

If it is assumed that the qubit is not undergoing any coherent evolution ( $H = 0$ ), i.e. a memory stage within

a quantum algorithm, then Eq. 56 can be solved by re-expressing the density matrix in the Bloch formalism. Set  $\rho(t) = I/2 + x(t)X + y(t)Y + z(t)Z$ , then Eq. 56, with  $H = 0$ , reduces to,  $\partial_t S(t) = A S(t)$  with  $S(t) = (x(t), y(t), z(t))^T$  and

$$A = \begin{pmatrix} -(\Gamma + 2\Gamma_Z) & 0 & 0 \\ 0 & -(\Gamma + 2\Gamma_Z) & 0 \\ 0 & 0 & -2\Gamma \end{pmatrix}. \quad (57)$$

This differential equation is easy to solve, leading to,

$$\begin{aligned} \rho(t) = [1 - p(t)]\rho(0) + p_x(t)X\rho(0)X \\ + p_y(t)Y\rho(0)Y + p_z(t)Z\rho(0)Z, \end{aligned} \quad (58)$$

where,

$$\begin{aligned} p_x(t) = p_y(t) &= \frac{1}{4}(1 - e^{-2\Gamma t}), \\ p_z(t) &= \frac{1}{4}(1 + e^{-2\Gamma t} - 2e^{-(\Gamma + 2\Gamma_Z)t}), \\ p(t) &= p_x(t) + p_y(t) + p_z(t). \end{aligned} \quad (59)$$

If this single qubit is part of a QEC encoded data block, then each term represents a single error on the qubit experiencing decoherence. Two blocks of initialized ancilla qubits are added to the system and the error correction protocol run. Once the ancilla qubits are measured, the state will collapse to no error, with probability  $1 - p(t)$ , or a single  $X, Y$  or  $Z$  error, with probabilities  $p_x(t), p_y(t)$  and  $p_z(t)$ .

We can also see how temporal effects are incorporated into the error correction model. The temporal integration window  $t$  of the master equation will influence how probable an error is detected and corrected for a fixed rate  $\Gamma$ . The longer between correction cycles, the more probable the qubit experiences an error.



### C. More General mappings

Both the systematic gate errors and the errors induced by environmental decoherence illustrate the digitization effect of quantum error correction. However, we can quite easily generalize digitization to arbitrary mappings of the density matrix. In this case consider a more general Krauss map on a multi-qubit density matrix,

$$\rho \rightarrow \sum_k A_k^\dagger \rho A_k \quad (60)$$

where  $\sum_k A_k^\dagger A_k = I$ . For the sake of simplicity let us choose a simple mapping where  $A_1 = (Z_1 + iZ_2)/\sqrt{2}$  and  $A_k = 0$  for  $k \neq 1$ . This mapping essentially represents dephasing on two qubits. However, this type of mapping (when considered in the context of error correction) represents independent  $Z$  errors on either qubit one or

two.

To illustrate, first expand out the density matrix (neglecting normalization),

$$\rho \rightarrow A_1^\dagger \rho A_1 = Z_1 \rho Z_1 + Z_2 \rho Z_2 - iZ_1 \rho Z_2 + iZ_2 \rho Z_1 \quad (61)$$

Note that only the first two terms in this expansion, on their own, represent physical mixtures, the last two off-diagonal terms are actually irrelevant in the context of QEC and are removed during correction. To illustrate we again assume that  $\rho$  represents a protected qubit, where  $Z_1$  and  $Z_2$  are *physical* errors on qubits comprising the codeblock. As we are only considering phase errors in this example, we will ignore  $X$  correction (but the analysis automatically generalizes if the error mapping contains  $X$  terms). A fresh ancilla block, represented by the density matrix  $\rho_0^z$  is coupled to the system and the unitary  $U_{QEC}$  is run,

$$\begin{aligned} U_{QEC}^\dagger \rho' \otimes \rho_0^z U_{QEC} &= U_{QEC}^\dagger Z_1 \rho Z_1 \otimes \rho_0^z U_{QEC} + U_{QEC}^\dagger Z_2 \rho Z_2 \otimes \rho_0^z U_{QEC} \\ &\quad - iU_{QEC}^\dagger Z_1 \rho Z_2 \otimes \rho_0^z U_{QEC} + iU_{QEC}^\dagger Z_2 \rho Z_1 \otimes \rho_0^z U_{QEC} \\ &= Z_1 \rho Z_1 \otimes |Z_1\rangle \langle Z_1| + Z_2 \rho Z_2 \otimes |Z_2\rangle \langle Z_2| - iZ_1 \rho Z_2 \otimes |Z_1\rangle \langle Z_2| + iZ_2 \rho Z_1 \otimes |Z_2\rangle \langle Z_1| \end{aligned} \quad (62)$$

where  $|Z_1\rangle$  and  $|Z_2\rangle$  represent the two orthogonal syndrome states of the ancilla that are used to detect phase errors on qubits one and two respectively. The important part of the above expression is that when the syndrome qubits are measured we are calculating  $\text{Tr}(\rho |Z_1\rangle \langle Z_1|)$  or  $\text{Tr}(\rho |Z_2\rangle \langle Z_2|)$ , therefore the two cross terms in the above expression are never observed. In this mapping the only two possible states that exist after the measurement of the ancilla system are,

$$\begin{aligned} Z_1 \rho Z_1 \otimes |Z_1\rangle \langle Z_1| \quad \text{with Probability} &= \frac{1}{2} \\ Z_2 \rho Z_2 \otimes |Z_2\rangle \langle Z_2| \quad \text{with Probability} &= \frac{1}{2} \end{aligned} \quad (63)$$

Therefore, not only are the cross terms eliminated via error correction but the final density matrix again collapses to a single error perturbation of “clean” codeword states with no correlated errors.

Consequently, in standard QEC analysis it is assumed that after each elementary gate operation, measurement, initialization and memory step, a hypothetical error correction cycle is run. This cycle digitizes all continuous errors (either systematic or environmental) into either an  $X$  and/or  $Z$  error on each qubit. This cycle is assumed to be error free and take zero time. In this way error correction can be analyzed by assuming perfect gate operations and discrete, probabilistic errors. The probability of each error occurring can then be independently calculated via a systematic gate analysis or through the evolution of the master equation.

### X. FAULT-TOLERANT QUANTUM ERROR CORRECTION AND THE THRESHOLD THEOREM.

Section VII detailed the protocols required to correct for quantum errors, however this implementation of QEC assumed the following,

1. Errors only occur during “memory” regions, i.e. when quantum operations or error correction are not being performed and we assume errors do not occur on ancilla qubits.
2. The quantum gates themselves do not induce any systematic errors within the logical data block.

Clearly these are two very unrealistic assumptions and error correction procedures and logical gate operations need to be designed such that they can still correct for errors.

#### A. Fault-tolerance

The concept of Fault-tolerance in computation is not a new idea, it was first developed in relation to classical computing (Neu55; G83; Avi87). However, in recent years the precise manufacturing of digital circuitry has made large scale error correction and fault-tolerant circuits largely unnecessary.

The basic principle of Fault-tolerance is that the circuits used for gate operations and error correction pro-

cedures should not cause errors to cascade. This can be seen clearly when we look at a simple CNOT operation between two qubits [Fig. 10]. In this circuit we are performing a sequence of three CNOT gates which act to take the state  $|111\rangle|000\rangle \rightarrow |111\rangle|111\rangle$ . In Fig. 10a. we consider a single  $X$  error which occurs on the top most qubit prior to the first CNOT. This single error will cascade through each of the three gates such that the  $X$  error has now propagated to four qubits. Fig. 10b. shows a slightly modified design that implements the same operation, but the single  $X$  error now only propagates to two of the six qubits. If we consider each block of three as a single logical qubit, then the staggered circuit will only induce a total of one error in each logical block, given a single  $X$  error occurred somewhere during the gate operations. This is the one of the standard definitions of Fault-tolerance.

*fault-tolerant circuit element: A single error will cause at most one error in the output for each logical qubit block.*

It should be stressed that the idea of Fault-tolerance is a discrete definition, either a certain quantum operation is fault-tolerant or it is not. What is defined to be fault-tolerant can change depending on the error correction code used. For example, for a single error correcting code, the above definition is the only one available (since any more than one error in a logical qubit will result in the error correction procedure failing). However, if the quantum code employed is able to correct multiple errors, then the definition of Fault-tolerance can be relaxed, i.e. if the code can correct three errors then circuits may be designed such that a single failure results in at most two errors in the output (which is then correctable). In general, for an code correcting  $t = \lfloor (d-1)/2 \rfloor$  errors, fault-tolerance requires that  $\leq t$  errors during an operation does not result in  $> t$  errors in the output for each logical qubit.

## B. Threshold Theorem

The threshold theorem is truly a remarkable result in quantum information and is a consequence of fault-tolerant circuit design and the ability to perform dynamical error correction. Rather than present a detailed derivation of the theorem for a variety of noise models, we will instead take a very simple case where we utilize a quantum code that can only correct for a single error, using a model that assumes uncorrelated, errors on individual qubits. For more rigorous derivations of the theorem see (ABO97; Got97; Ali07).

Consider a quantum computer where each physical qubit experiences either an  $X$  and/or  $Z$  error independently with probability  $p$ , per gate operation. Furthermore, it is assumed that each logical gate operation and error correction circuit is designed according to the rules of Fault-tolerance and that a cycle of error correction is performed after each elementary *logical* gate operation.

If an error occurs during a logical gate operation, then Fault-tolerance ensures this error will only propagate to at most one error in each block, after which a cycle of error correction will remove the error. Hence if the failure probability of un-encoded qubits per time step is  $p$ , then a single level of error correction will ensure that the logical step fails only when two (or more) errors occur. Hence the failure rate of each logical operation, to leading order, is now  $p_L^1 = cp^2$ , where  $p_L^1$  is the failure rate (per logical gate operation) of a 1st level logical qubit and  $c$  is the upper bound for the number of possible 2-error combinations which can occur at a physical level within the circuit consisting of the correction cycle + gate operation + correction cycle (Ali07). We now repeat the process, re-encoding the computer such that a level-2 logical qubit is formed, using the same  $[[n, k, d]]$  quantum code, from  $n$ , level-1 encoded qubits. It is assumed that all error correcting procedures and gate operations at the 2nd level are self-similar to the level-1 operations (i.e. the circuit structures for the level-2 encoding are identical to the level-1 encoding). Therefore, if the level-1 failure rate per logical time step is  $p_L^1$ , then by the same argument, the failure rate of a 2-level operation is given by,  $p_L^2 = c(p_L^1)^2 = c^3p^4$ . This iterative procedure is then repeated (referred to as concatenation) up to the  $k$ th level, such that the logical failure rate, per time step, of a  $k$ -level encoded qubit is given by,

$$p_L^k = \frac{(cp)^{2^k}}{c}. \quad (64)$$

Eq. 64 implies that for a finite *physical* error rate,  $p$ , per qubit, per time step, the failure rate of the  $k$ th-level encoded qubit can be made arbitrarily small by simply increasing  $k$ , dependent on  $cp < 1$ . This inequality defines the threshold. The physical error rate experienced by each qubit per time step must be  $p_{th} < 1/c$  to ensure that multiple levels of error correction reduce the failure rate of logical components.

Hence, provided sufficient resources are available, an arbitrarily large quantum circuit can be successfully implemented, to arbitrary accuracy, once the physical error rate is below threshold. The calculation of thresholds is therefore an extremely important aspect to quantum architecture design. Initial estimates at the threshold, which gave  $p_{th} \approx 10^{-4}$  (Kit97; ABO97; Got97) did not sufficiently model physical systems in an accurate way. Recent results (SFH08; SDT07; SBF<sup>+</sup>06; MCT<sup>+</sup>04; BKSO05) have been estimated for more realistic quantum processor architectures, showing significant differences in threshold when architectural considerations are taken into account.

## XI. FAULT-TOLERANT OPERATIONS ON ENCODED DATA

Sections VII and X showed how fault-tolerant QEC allows for any quantum algorithm to be run to arbitrary

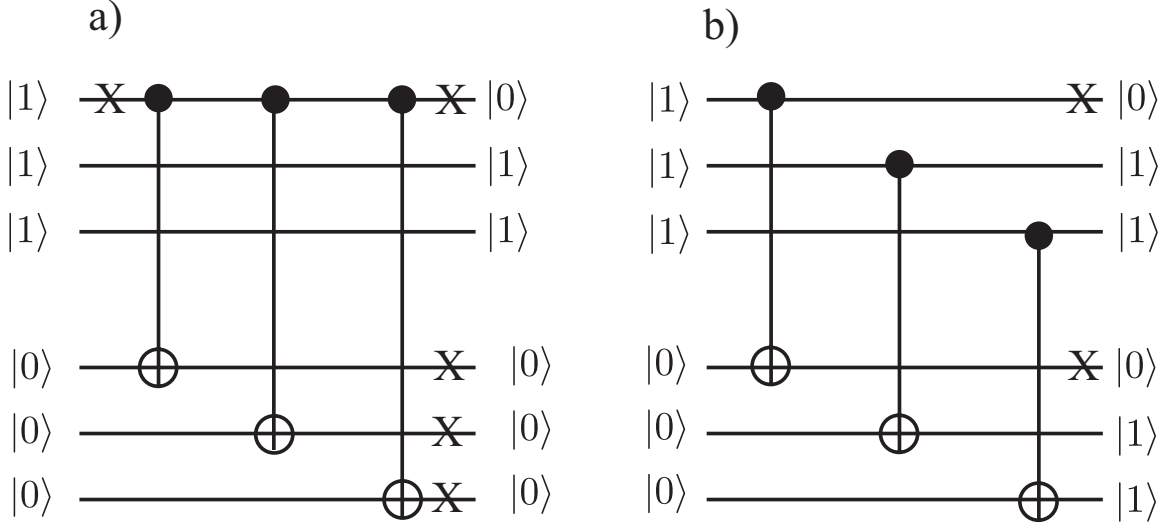


FIG. 10 Two circuits to implement the transformation  $|111\rangle|000\rangle \rightarrow |111\rangle|111\rangle$ . a) shows a version where a single  $X$  error can cascade into four errors while b) shows an equivalent circuit where the error only propagates to a second qubit.

accuracy. However, the results of the threshold theorem assume that logical operations can be performed directly on the encoded data without the need for continual decoding and re-encoding. Using stabilizer codes, a large class of operations can be performed on logical data in an inherently fault-tolerant way.

If a given logical state,  $|\psi\rangle_L$ , is stabilized by  $K$ , and the logical operation  $U$  is applied, the new state,  $U|\psi\rangle_L$  is stabilized by  $UKU^\dagger$ , i.e.,

$$UKU^\dagger U|\psi\rangle_L = UK|\psi\rangle_L = U|\psi\rangle_L. \quad (65)$$

In order for the codeword states to remain valid, the stabilizer set for the code,  $\mathcal{G}$ , must remain fixed through every operation. Hence for  $U$  to be a valid operation on the data,  $UGU^\dagger = \mathcal{G}$ .

### A. Single Qubit Operations

The logical  $\bar{X}$  and  $\bar{Z}$  operations on a single encoded qubit are the first examples of valid codeword operations. Taking the  $[[7, 1, 3]]$  code as an example,  $\bar{X}$  and  $\bar{Z}$  are given by,

$$\bar{X} = XXXXXXX \equiv X^{\otimes 7}, \quad \bar{Z} = ZZZZZZZ \equiv Z^{\otimes 7}. \quad (66)$$

Since the single qubit Pauli operators satisfy  $XZX = -Z$  and  $ZXZ = -X$  then,  $\bar{X}K^i\bar{X} = K^i$  and  $\bar{Z}K^i\bar{Z} = K^i$  for each of the  $[[7, 1, 3]]$  stabilizers given in Eq. 44. The fact that each stabilizer has a weight of four guarantees that  $UKU^\dagger$  picks up an even number of  $-1$  factors. Since the stabilizers remain fixed the operations are valid. However, what transformations do Eq. 66 actually perform on encoded data?

For a single qubit, a bit-flip operation  $X$  takes  $|0\rangle \leftrightarrow |1\rangle$ . Recall that for a single qubit  $Z|0\rangle = |0\rangle$  and

$Z|1\rangle = -|1\rangle$ , hence for  $\bar{X}$  to actually induce a logical bit-flip it must take,  $|0\rangle_L \leftrightarrow |1\rangle_L$ . For the  $[[7, 1, 3]]$  code, the final operator which fixes the logical state is  $K^7 = Z^{\otimes 7}$ , where  $K^7|0\rangle_L = |0\rangle_L$  and  $K^7|1\rangle_L = -|1\rangle_L$ . As  $\bar{X}K^7\bar{X} = -K^7$ , any state stabilized by  $K^7$  becomes stabilized by  $-K^7$  (and vice-versa) after the operation of  $\bar{X}$ . Therefore,  $\bar{X}$  represents a logical bit flip. The same argument can be used for  $\bar{Z}$  by considering the stabilizer properties of the states  $|\pm\rangle = (|0\rangle \pm |1\rangle)/\sqrt{2}$ . Hence, the logical bit- and phase-flip gates can be applied directly to logical data by simply using seven single qubit  $X$  or  $Z$  gates, [Fig. 11].

Two other useful gates which can be applied in this manner is the Hadamard rotation and phase gate,

$$H = \frac{1}{\sqrt{2}} \begin{pmatrix} 1 & 1 \\ 1 & -1 \end{pmatrix}, \quad P = \begin{pmatrix} 1 & 0 \\ 0 & i \end{pmatrix}. \quad (67)$$

These gates are useful since when combined with the two-qubit CNOT gate, they can generate a subgroup of all multi-qubit gates known as the Clifford group (gates which map Pauli group operators back to the Pauli group). Again, using the stabilizers of the  $[[7, 1, 3]]$  code and the fact that for single qubits,

$$\begin{aligned} HXH &= Z, & HZH &= X, \\ PXP^\dagger &= iXZ, & PZP^\dagger &= Z, \end{aligned} \quad (68)$$

a seven qubit bit-wise Hadamard gate will switch  $X$  with  $Z$  and therefore will simply flip  $\{K^1, K^2, K^3\}$  with  $\{K^4, K^5, K^6\}$ , and is a valid operation. The bit-wise application of the  $P$  gate will leave any  $Z$  stabilizer invariant, but takes  $X \rightarrow iXZ$ . This is still valid since provided there are a multiple of four non-identity operators for the stabilizer set, the factors of  $i$  will cancel. Hence seven bit-wise  $P$  gates is valid for the  $[[7, 1, 3]]$  code.

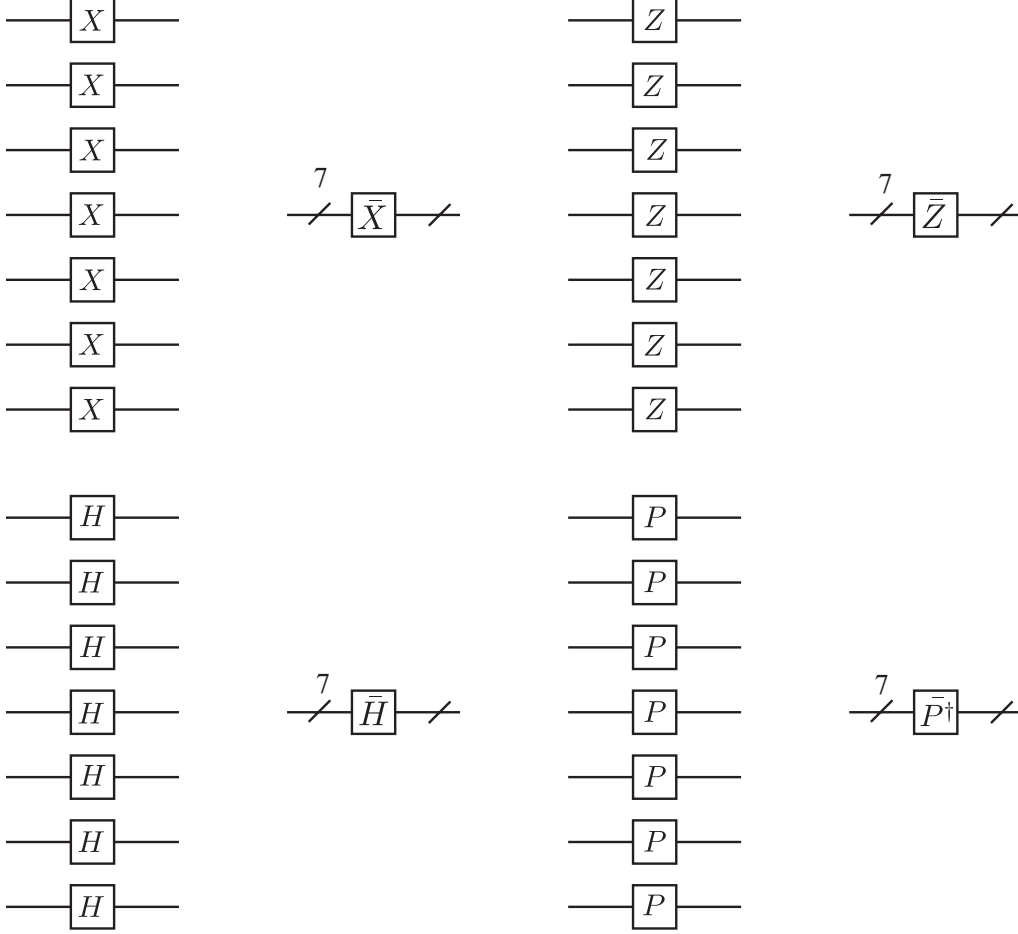


FIG. 11 Bit-wise application of single qubit gates in the  $[[7, 1, 3]]$  code. Logical  $X$ ,  $Z$ ,  $H$  and  $P$  gates can trivially be applied by using seven single qubit gates, fault-tolerantly. Note that the application of seven  $P$  gates results in the logical  $\bar{P}^\dagger$  being applied and vice-versa.

What does  $\bar{H}$  and  $\bar{P}$  do to the logical state? For a single qubit, the Hadamard gate flips any  $Z$  stabilized state to a  $X$  stabilized state, i.e.  $|0, 1\rangle \leftrightarrow |+, -\rangle$ . Looking at the transformation of  $K^7$ ,  $\bar{H}K^7\bar{H} = X^{\otimes 7}$ , the bit-wise Hadamard gate will invoke a logical Hadamard operation. The single qubit  $P$  gate leaves a  $Z$  stabilized state invariant, while an  $X$  eigenstate becomes stabilized by  $iXZ$ . Hence,  $\bar{P}^\dagger(X^{\otimes 7})\bar{P} = -i(XZ)^{\otimes 7}$  and the bit-wise gate,  $\bar{P}$ , represents a logical  $P^\dagger$  gate on the data block. Similarly, bit-wise  $\bar{P}^\dagger$  gates enact a logical  $P$  gate [Fig. 11]. Each of these fault-tolerant operations on a logically encoded block are commonly referred to as transversal operations, as a logical operation is obtained by a set of individual operations acting transversally on the physical qubits.

## B. Two-qubit gate.

A two-qubit logical CNOT operation can also be applied in the same transversal way. For un-encoded qubits, a CNOT operation performs the following mapping on

the two qubit stabilizer set,

$$\begin{aligned} X \otimes I &\rightarrow X \otimes X, \\ I \otimes Z &\rightarrow Z \otimes Z, \\ Z \otimes I &\rightarrow Z \otimes I, \\ I \otimes X &\rightarrow I \otimes X. \end{aligned} \tag{69}$$

Where the first operator corresponds to the control qubit and the second operator corresponds to the target. Now consider the bit-wise application of seven CNOT gates between logically encoded blocks of data [Fig. 12]. First the stabilizer set must remain invariant, i.e.,

$$\mathcal{G} = \{K^i \otimes K^j\} \rightarrow \{K^i \otimes K^j\} \forall (i, j). \tag{70}$$

Table V details the transformation for all the stabilizers under seven bit-wise CNOT gates, demonstrating that this operation is valid on the  $[[7, 1, 3]]$  code. The transformations in Eq. 69 are trivially extended to the logical space, showing that seven bit-wise CNOT gates invoke a

logical CNOT operation.

$$\begin{aligned}
 \bar{X} \otimes I &\rightarrow \bar{X} \otimes \bar{X}, \\
 I \otimes \bar{Z} &\rightarrow \bar{Z} \otimes \bar{Z}, \\
 \bar{Z} \otimes I &\rightarrow \bar{Z} \otimes I, \\
 I \otimes \bar{X} &\rightarrow I \otimes \bar{X}.
 \end{aligned} \tag{71}$$

The issue of Fault-tolerance with these logical operations should be clear. The  $\bar{X}, \bar{Z}, \bar{H}$  and  $\bar{P}$  gates are trivially fault-tolerant since the logical operation is performed through seven bit-wise single qubit gates. The logical CNOT is also fault-tolerant since each two-qubit gate only operates between counterpart qubits in each logical block. Hence if any gate is inaccurate, then at most a single error will be introduced in each block.

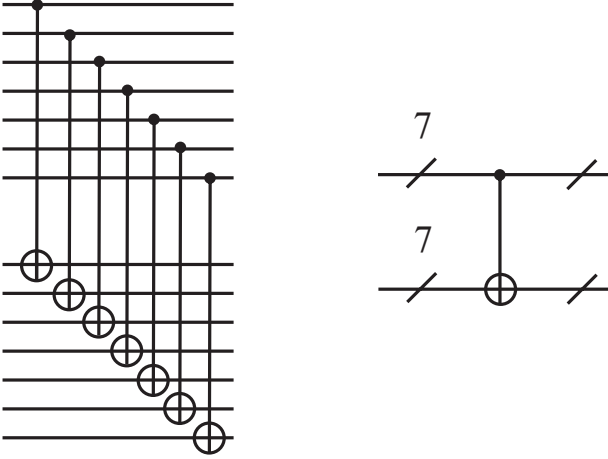


FIG. 12 Bit-wise application of a CNOT gate between two logical qubits. Since each CNOT only couples corresponding qubits in each block, this operation is inherently fault-tolerant.

In contrast to the  $[[7,1,3]]$  code, let us also take a quick look at the  $[[5,1,3]]$  code. As mentioned in section VIII the  $[[5,1,3]]$  code is a non-CSS code, meaning the Clifford group of gates cannot be fully implemented in a transversal manner. To see this clearly we can examine how the stabilizer group for the code transforms under a transversal Hadamard operation,

$$\begin{pmatrix} X & Z & Z & X & I \\ I & X & Z & Z & X \\ X & I & X & Z & Z \\ Z & X & I & X & Z \end{pmatrix} \rightarrow \begin{pmatrix} Z & X & X & Z & I \\ I & X & X & X & Z \\ Z & I & Z & X & X \\ X & Z & I & Z & X \end{pmatrix} \tag{72}$$

The stabilizer group is not preserved under this transformation, therefore the transversal Hadamard operation is not valid for the  $[[5,1,3]]$  code. One thing to briefly note is that there is a method for performing logical Hadamard and phase gates on the  $[[5,1,3]]$  code (Got97). However, it essentially involves performing a valid, transversal, three-qubit gate and then measuring out two of the logical ancillae.

While these gates are useful for operating on quantum data, they do not represent a universal set for quantum computation. In fact it has been shown that by using the stabilizer formalism, these operations can be efficiently simulated on a classical device (Got98; AG04). In order to achieve universality one of the following gates are generally added to the available set,

$$T = \begin{pmatrix} 1 & 0 \\ 0 & e^{i\pi/4} \end{pmatrix}, \tag{73}$$

or the Toffoli gate (Tof81). However, neither of these two gates are members of the Clifford group and applying them in a similar way to the other gates will transform the stabilizers out the group and consequently does not represent a valid operation. Circuits implementing these two gates in a fault-tolerant manner have been developed (NC00; GC99; SI05; SFH08), but at this stage the circuits are complicated and resource intensive. This has practical implications to encoded operations. If universality is achieved by adding the  $T$  gate to the list, arbitrary single qubit rotations require long gate sequences (utilizing the Solovay-Kitaev theorem (Kit97; DN06)) to approximate arbitrary logical qubit rotations and these sequences often require many  $T$  gates (Fow05). Finding more efficient methods to achieve universality on encoded data is therefore still an active area of research.

## XII. FAULT-TOLERANT CIRCUIT DESIGN FOR LOGICAL STATE PREPARATION

Section X introduced the basic rules for fault-tolerant circuit design and how these rules lead to the threshold theorem for concatenated error correction. However, what does a full fault-tolerant quantum circuit look like? Here, we introduce a full fault-tolerant circuit to prepare the  $[[7, 1, 3]]$  logical  $|0\rangle$  state. As the  $[[7, 1, 3]]$  code is a single error correcting code, we use the one-to-one definition of Fault-tolerance and therefore only need to consider the propagation of a single error during the preparation (any more that one error during correction represents a higher order effect and is ignored).

As described in Section VII, logical state preparation can be done by initializing an appropriate number of physical qubits and measuring each of the  $X$  stabilizers that describe the code. Therefore, a circuit which allows the measurement of a Hermitian operator in a fault-tolerant manner needs to be constructed. The general structure of the circuit used was first developed by Shor (Sho96), however it should be noted that several more recent methods for fault-tolerant state preparation and correction now exist (Ste97a; Ste02; DA07) which are more efficient than Shor's original method.

The circuits shown in Fig. 13a and 13b, which measure the stabilizer  $K^1 = IIIXXXX$  are not fault-tolerant, since a single ancilla is used to control each of the four CNOT gates. Instead, four ancilla qubits are used which are prepared in the state  $|\mathcal{A}\rangle = (|0000\rangle + |1111\rangle)/\sqrt{2}$ .

$K^i \otimes K^j$	$K^1$	$K^2$	$K^3$	$K^4$	$K^5$	$K^6$
$K^1$	$K^1 \otimes I$	$K^1 \otimes K^1 K^2$	$K^1 \otimes K^1 K^3$	$K^1 K^4 \otimes K^1 K^4$	$K^1 K^5 \otimes K^1 K^5$	$K^1 K^6 \otimes K^1 K^6$
$K^2$	$K^2 \otimes K^1 K^2$	$K^2 \otimes I$	$K^2 \otimes K^2 K^3$	$K^2 K^4 \otimes K^2 K^4$	$K^2 K^5 \otimes K^2 K^5$	$K^2 K^6 \otimes K^2 K^6$
$K^3$	$K^3 \otimes K^3 K^1$	$K^3 \otimes K^3 K^2$	$K^3 \otimes I$	$K^3 K^4 \otimes K^3 K^4$	$K^3 K^5 \otimes K^3 K^5$	$K^3 K^6 \otimes K^3 K^6$
$K^4$	$K^4 \otimes K^1$	$K^4 \otimes K^2$	$K^4 \otimes K^3$	$I \otimes K^4$	$K^4 K^5 \otimes K^5$	$K^4 K^6 \otimes K^6$
$K^5$	$K^5 \otimes K^1$	$K^5 \otimes K^2$	$K^5 \otimes K^3$	$K^5 K^4 \otimes K^4$	$I \otimes K^5$	$K^5 K^6 \otimes K^6$
$K^6$	$K^6 \otimes K^1$	$K^6 \otimes K^2$	$K^6 \otimes K^3$	$K^6 K^4 \otimes K^4$	$K^6 K^5 \otimes K^5$	$I \otimes K^6$

TABLE V Transformations of the  $[[7, 1, 3]]$  stabilizer set under the gate operation  $U = \text{CNOT}^{\otimes 7}$ , where  $\mathcal{G} \rightarrow U^\dagger \mathcal{G} U$ . Note that the transformation does not take any stabilizer outside the group generated by  $K^i \otimes K^j$  ( $i, j \in [1, \dots, 6]$ ), therefore  $U = \text{CNOT}^{\otimes 7}$  represents a valid operation on the codespace.

This can be done by initializing four qubits in the  $|0\rangle$  state and applying a Hadamard then a sequence of CNOT gates. Each of these four ancilla are used to control a separate CNOT gate, after which the ancilla state is decoded and measured. By ensuring that each CNOT is controlled via a separate ancilla, any  $X$  error will only propagate to a single qubit in the data block. However, during the preparation of the ancilla state there is the possibility that a single  $X$  error can propagate to multiple ancilla, which are then fed forward into the data block. In order to combat this, the ancilla block needs to be verified against possible  $X$  errors. Tracking through all the possible locations where a single  $X$  error can occur during ancilla preparation leads to the following unique states.

$$\begin{aligned}
|\mathcal{A}\rangle_1 &= \frac{1}{\sqrt{2}}(|0000\rangle + |1111\rangle), \\
|\mathcal{A}\rangle_2 &= \frac{1}{\sqrt{2}}(|0001\rangle + |1110\rangle), \\
|\mathcal{A}\rangle_3 &= \frac{1}{\sqrt{2}}(|0011\rangle + |1100\rangle), \\
|\mathcal{A}\rangle_4 &= \frac{1}{\sqrt{2}}(|0111\rangle + |1000\rangle), \\
|\mathcal{A}\rangle_5 &= \frac{1}{\sqrt{2}}(|0100\rangle + |1011\rangle).
\end{aligned} \tag{74}$$

From these possibilities, the last four states have a different parity between the first and forth qubit. Hence to verify this state, a fifth ancilla is added, initialized and used to perform a parity check on the ancilla block. This fifth ancilla is then measured. If the result is  $|0\rangle$ , the ancilla block is clean and can be coupled to the data. If the ancilla result is  $|1\rangle$ , then either a single error has occurred in the ancilla preparation or on this verification qubit. In either case, the entire ancilla block is re-initialized and the ancilla prepared again. This is continued until the verification qubit is measured to be  $|0\rangle$  [Fig. 14]. The re-preparation of the ancilla block protects against  $X$  errors, which can propagate forward through the CNOT gates.  $Z$  errors on the other hand, propagate in the other direction. Any  $Z$  error which occurs in the ancilla block will propagate straight through to the final measurement. This results in the measurement not corresponding to the eigenstate the data is projected to and can possibly result in mis-correction once all stabilizers have been measured.

To protect against this, each stabilizer is measured 2-3 times and a majority vote of the measurement results taken. As any additional error represents a second order process, if the first or second measurement has been corrupted by an induced  $Z$  error, then the third measurement will only contain additional errors if a higher order error process has occurred. Therefore, we are free to ignore this possibility and assume that the third measurement is error free. The full circuit for  $[[7, 1, 3]]$  state preparation is shown in Fig. 15, where each stabilizer is measured 2-3 times. The total circuit requires a minimum of 12 qubits (7-data qubits and a 5-qubit ancilla block).

As you can see, the circuit constructions for full fault-tolerant state preparation (and error correction) are not simple circuits. However, they are easy to design in generic ways when employing stabilizer coding.

### XIII. LOSS PROTECTION

So far we have focused the discussion on correction techniques which assume that error processes maintain the assumption of a qubit structure to the Hilbert space. As we noted in section III.C, the loss of physical qubits within the computer violates this assumption and in general requires additional correction machinery beyond what we have already discussed.

For the sake of completeness, this section examines some correction techniques for qubit loss. Specifically, we detail one such scheme which was developed with single photon based architectures in mind.

Protecting against qubit loss requires a different approach than other general forms of quantum errors such as environmental decoherence or systematic control imperfections. The cumbersome aspect related to correcting qubit loss is detecting the presence of a qubit at the physical level. The specific machinery that is required for loss detection is dependent on the underlying physical architecture, but the basic principal is that the presence or absence of the physical qubit must be determined without discriminating the actual quantum state.

Certain systems allow for loss detection is a more convenient way than others. Electronic spin qubits, for example, can employ Single Electron Transistors (SET) to detect the presence or absence of the charge

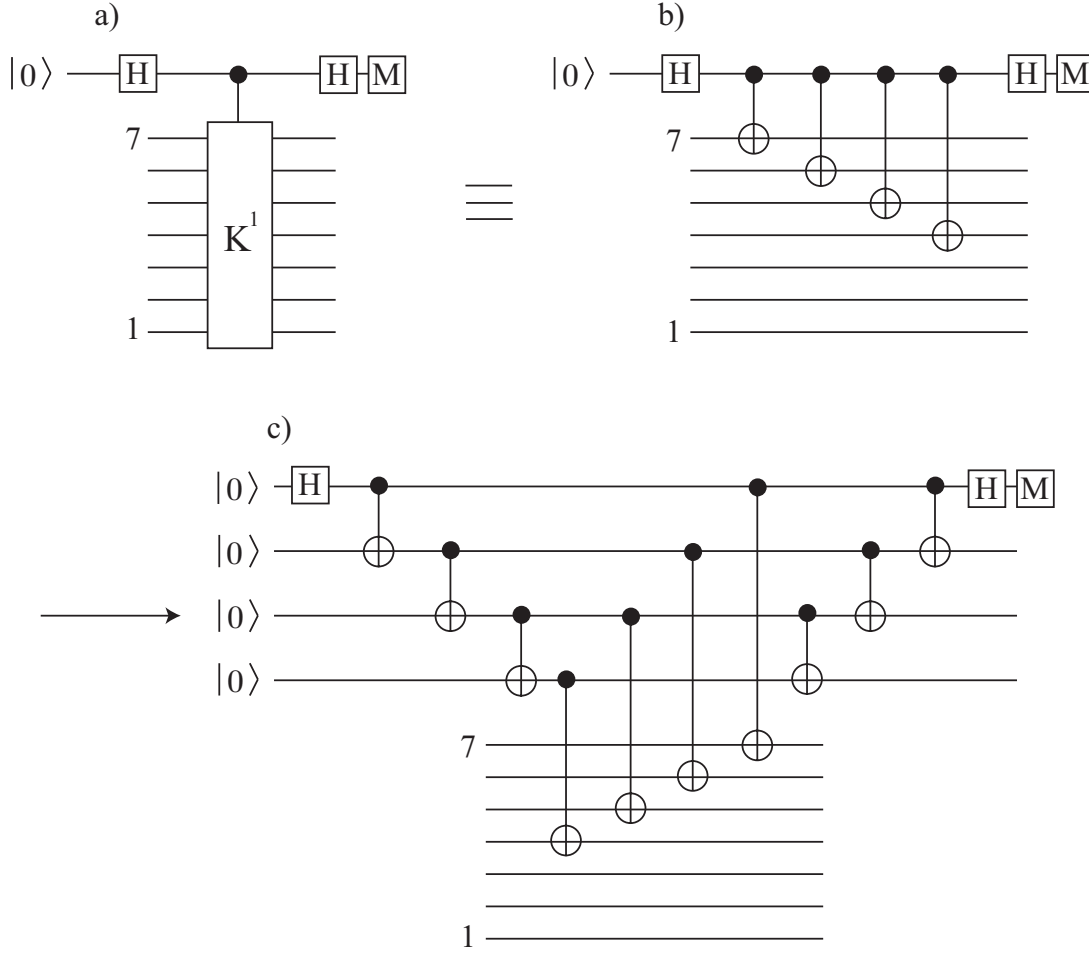


FIG. 13 Three circuits which measure the stabilizer  $K^1$ . Fig a) represents a generic operator measurement where a multi-qubit controlled gate is available. Fig. b) decomposes this into single- and two-qubit gates, but in a non-fault-tolerant manner. Fig. c) introduces four ancilla such that each CNOT is controlled via a separate qubit. This ensures Fault-tolerance.

without performing measurement on the spin degree of freedom (DS00; CGJH05; AJW<sup>+</sup>01). Optics in contrast requires more complicated non-demolition measurement (MW84; IHY85; POW<sup>+</sup>04; MNBS05). This is due to the fact that typical photonic measurement is performed via photo-detectors which have the disadvantage of physically destroying the photon.

Once the detection of the presence of the physical qubit has been performed, a freshly initialized qubit can be injected to replace the lost qubit. Once this has been completed, the standard error correcting procedure can correct for the error. A freshly initialized qubit state,  $|0\rangle$  can be represented as projective collapse of a general qubit state,  $|\psi\rangle$ , as,

$$|0\rangle \propto |\psi\rangle + Z|\psi\rangle. \quad (75)$$

If we consider this qubit as part of an encoded block, then the above corresponds to a 50% error probability of experiencing a phase flip on this qubit. Therefore, a loss event that is corrected by non-demolition detection and

standard QEC essentially guarantees a correction event in the QEC cycle. Therefore the probability of loss needs to be at a comparable rate to standard errors as the correction cycle after a loss detection event will, with high probability, detect and correct the error.

Additionally, if a loss event is detected and the qubit replaced, the error detection code shown in section VI becomes a single qubit correction code. This is due to the fact that erasure errors have known locations. Consequently error detection is sufficient to perform full correction, in contrast to non-erasure errors where the location is unknown.

A second method for loss correction is related to systems that have high loss rates compared to systematic and environmental errors. The most prevalent in optical systems. Due to the high mobility of single photons and their relative immunity to environmental interactions, loss is a major error channel that generally dominates over other error sources. The use of error detection and correction codes for photon loss is unde-

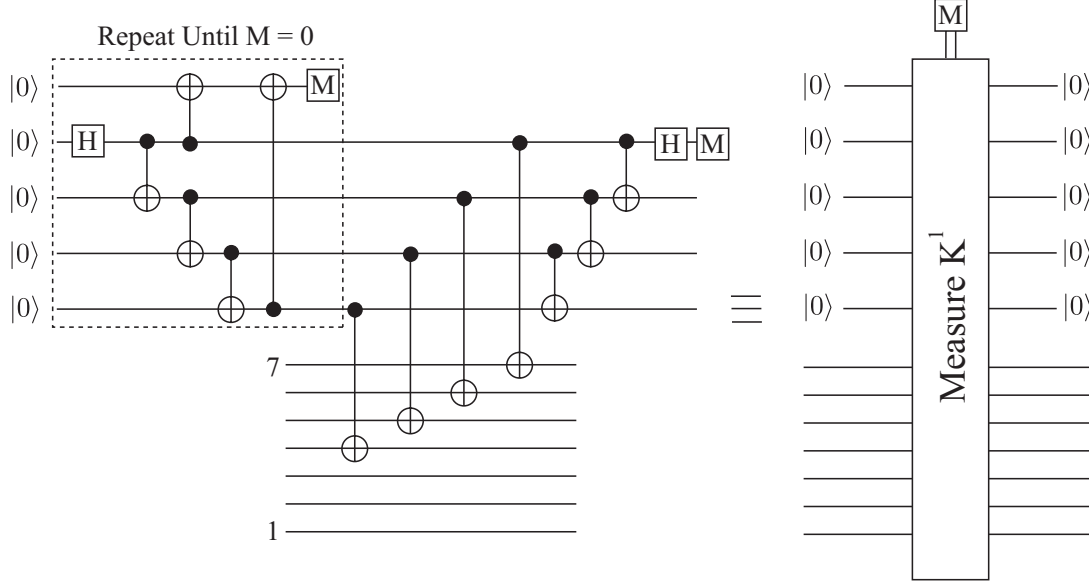


FIG. 14 Circuit required to measure the stabilizer  $K^1$ , fault-tolerantly. A four qubit GHZ state is used as ancilla with the state requiring verification against multiple  $X$  errors. After the state has passed verification it is coupled to the data block and a syndrome is extracted.

sirable due to the need for non-demolition detection of the lost qubit. While techniques exist for measuring the presence or absence of a photon without direct detection have been developed and implemented (POW<sup>+</sup>04), they require multiple ancilla photons and controlled interactions. Ultimately it is more desirable to redesign the loss correction code such that it can be employed directly with photo-detection rather than more complicated non-demolition techniques.

One such scheme was developed by Ralph, Hayes and Gilchrist in 2005 (RHG05). This scheme was a more efficient extension of an original Parity encoding method developed by Knill, Laflamme and Milburn to protect against photon loss in their controlled- $\sigma_z$  gate (KLM01). The general Parity encoding for a logical qubit is an  $N$  photon GHZ state in the conjugate basis, i.e.,

$$\begin{aligned} |0\rangle_L^N &= \frac{1}{\sqrt{2}}(|+\rangle^{\otimes N} + |-\rangle^{\otimes N}), \\ |1\rangle_L^N &= \frac{1}{\sqrt{2}}(|+\rangle^{\otimes N} - |-\rangle^{\otimes N}), \end{aligned} \quad (76)$$

where  $|\pm\rangle = (|0\rangle \pm |1\rangle)/\sqrt{2}$ . The motivation with this type of encoding is that measuring any qubit in the  $|0, 1\rangle$  basis simply removes it from the state, reducing the re-

sulting state by one, i.e.,

$$\begin{aligned} P_{0,N} |0\rangle_L^N &= (I_N + Z_N) |0\rangle_L^N \\ &= \frac{1}{\sqrt{2}}(|+\rangle^{N-1} + |-\rangle^{N-1}) |0\rangle_N = |0\rangle_L^{N-1} |0\rangle_N \\ P_{1,N} |0\rangle_L^N &= (I_N - Z_N) |0\rangle_L^N \\ &= \frac{1}{\sqrt{2}}(|+\rangle^{N-1} - |-\rangle^{N-1}) |1\rangle_N = |1\rangle_L^{N-1} |1\rangle_N \end{aligned} \quad (77)$$

where  $P_{0,1,N}$  are the projectors corresponding to measurement in the  $|0, 1\rangle$  basis on the  $N^{\text{th}}$  qubit (up to normalization). The effect for the  $|1\rangle_L$  state is similar. Measuring the  $N^{\text{th}}$  qubit in the  $|0\rangle$  state simply removes it from the encoded state, reducing the logical zero state by one, while measuring the  $N^{\text{th}}$  qubit as  $|1\rangle$  enacts a logical bit flip at the same time as reducing the size of the logical state. However, since the measurement result is known, this encoded bit flip can be corrected for.

Instead of introducing the full scheme developed in (RHG05), we instead just give the general idea of how such encoding allows for loss detection without non-demolition measurements. Photon loss in this model is assumed equivalent to measuring the photon in the  $|0\rangle, |1\rangle$  basis, but not knowing the answer [Sec III.C]. Our ignorance of the measurement result could lead to a logical bit flip error on the encoded state, therefore we require the ability to protect against logical bit flip errors on the above states. As already shown, the 3-qubit code allows us to achieve such correction. Therefore the final step in this scheme is encoding the above states into a redundancy code (a generalized version of the 3-qubit code), where an arbitrary logical state,  $|\psi\rangle_L$  is now given



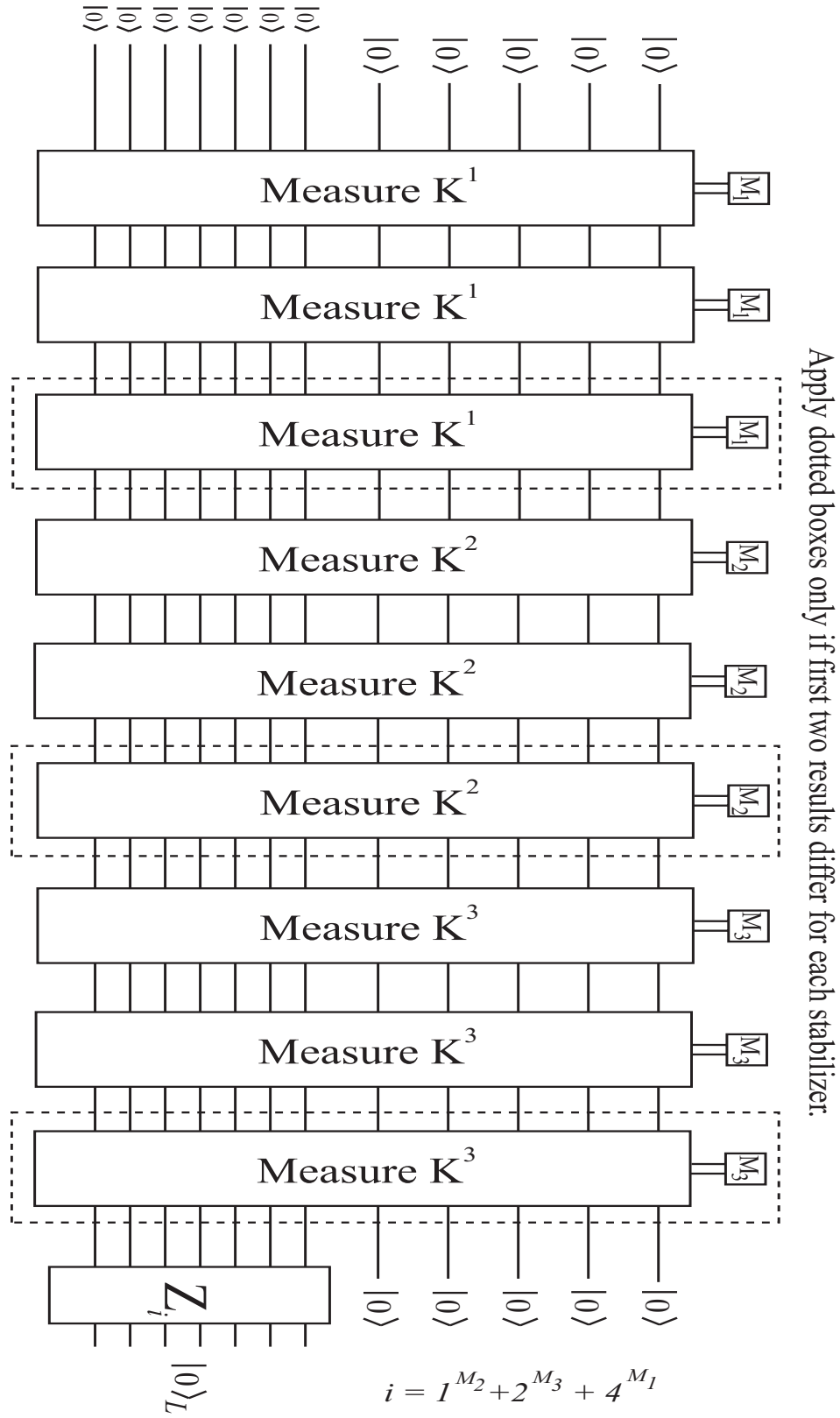


FIG. 15 Circuit required to prepare the  $[[7, 1, 3]]$  logical  $|0\rangle$  state fault-tolerantly. Each of the  $X$  stabilizers are sequentially measured using the circuit in Fig. 14. To maintain Fault-tolerance, each stabilizer is measured 2-3 times with a majority vote taken.

by,

$$|\psi\rangle_L = \alpha |0\rangle_1^N |0\rangle_2^N \dots |0\rangle_q^N + \beta |1\rangle_1^N |1\rangle_2^N \dots |1\rangle_q^N \quad (78)$$

where  $|0\rangle^N, |1\rangle^N$  are the parity encoded states shown in Eq. 77 and the fully encoded state is  $q$ -blocks of these parity states.

This form of encoding protects against the loss of qubits by first encoding the system into a code structure that allows for the removal of qubits without destroying the computational state and then protecting against logical errors that are induced by loss events. In effect it maps errors that are un-correctable by standard QEC to error channels that are correctable, in this case qubit loss  $\rightarrow$  qubit bit-flips. This is common with pathological error channels. If a specific type of error violates the standard “qubit” assumption of QEC, additional correction techniques are always required to map this type of error to a correctable form, consequently additional physical resources are usually needed.

#### XIV. SOME MODERN DEVELOPMENTS IN ERROR CORRECTION

Up until this stage we have restricted our discussions on error correction to the most basic principals and codes. The ideas and methodologies we have detailed represent the introductory techniques that were developed when error correction was first proposed. For those readers who are only looking for a basic introduction to the field, you can quite easily skip the remainder of this paper.

Providing a fair and encompassing review of the more modern and advanced error correction techniques that have been developed is far outside our goal for this review. However, we would be remiss if we did not briefly examine some of the more advanced error correction techniques that have been proposed for large scale quantum information processing. For the remainder of this discussion we choose two closely related error correction techniques, subsystem coding and topological coding which have been receiving significant attention in the fields of architecture design and large scale quantum information processing. While some readers may disagree, we review these two modern error correction protocols because they are currently two of the most useful correction techniques when discussing the physical construction of a quantum computer.

We again attempt to keep the discussion of these techniques light and provide specific examples when possible. However, it should be stressed that these error correcting protocols are far more complicated than the basic codes shown earlier. Topological error correction alone has since its introduction, essentially become its own research topic within the broader error correction field. Hence we encourage the reader who is interested to refer to the cited articles below for more rigorous and detailed treatment of these techniques.

#### A. Subsystem Codes

Quantum subsystem codes (Bac06) are one of the newer and highly flexible techniques to implement quantum error correction. The traditional stabilizer codes that we have reviewed are more formally identified as subspace codes, where information is encoded in a relevant coding subspace of a larger multi-qubit system. In contrast, subsystem coding identifies multiple subspaces of the multi-qubit system as equivalent for storing quantum information. Specifically, multiple states are identified with the logical  $|0\rangle_L$  and  $|1\rangle_L$  states.

The primary benefit to utilizing subsystem codes is the general nature of their construction. Moving from smaller to larger error correcting codes is conceptually straightforward, error correction circuits are much simpler to construct when encoding information in multiple subsystems (AC07) and the generality of their construction introduces the ability to perform dynamical code switching in a fault-tolerant manner (SEDH07). This final property gives subsystem coding significant flexibility as the strength of error correction within a quantum computer can be changed, fault-tolerantly, during operation of the device.

As with the other codes presented in this review, subsystem codes are stabilizer codes but now defined over a square lattice. The lattice dimensions represent the  $X$  and  $Z$  error correction properties and the size of the lattice in either of these two dimensions dictates the total number of errors the code can correct. In general, a  $\mathcal{C}(n_1, n_2)$  subsystem code is defined over a  $n_1 \times n_2$  square lattice which encodes one logical qubit into  $n_1 n_2$  physical qubits with the ability to correct at least  $\lfloor \frac{n_1-1}{2} \rfloor$   $Z$  errors and at least  $\lfloor \frac{n_2-1}{2} \rfloor$   $X$  errors. Again, keeping with the spirit of this review, we instead focus on a specific example, the  $\mathcal{C}(3,3)$  subsystem code. This code, encoding 9 physical qubits into one logical qubit can correct for one  $X$  and one  $Z$  error. In order to define the code structure we begin with a  $3 \times 3$  lattice of qubits, where each qubit is identified with the vertices of the lattice (note that this 2D structure represents the structure of the code, it does not imply that a physical array of qubits *must* be arranged into a 2D lattice). Fig. 16 illustrate three sets of stabilizer operators which are defined over the lattice. The first group, illustrated in Fig. 16a. is the stabilizer group,  $\mathcal{S}$ , which is generated by the operators,

$$\mathcal{S} = \langle X_{i,*} X_{i+1,*}; Z_{*,j} Z_{*,j+1} \mid i \in \mathbb{Z}_2; j \in \mathbb{Z}_2 \rangle, \quad (79)$$

where we retain the notation utilized in (AC07; SEDH07)  $U_{i,*}$  and  $U_{*,j}$  represent an operator,  $U$ , acting on all qubits in a given row,  $i$ , or column,  $j$ , respectively, and  $\mathbb{Z}_2 = \{1, 2\}$ . The second relevant subsystem is known as the gauge group [Fig. 16b.],  $\mathcal{T}$ , and is described via the non-Abelian group generated by the pairwise operators

$$\mathcal{T} = \langle X_{i,j} X_{i+1,j} \mid i \in \mathbb{Z}_2; j \in \mathbb{Z}_3 \rangle, \quad (80)$$

$$\langle Z_{i,j} Z_{i,j+1} \mid i \in \mathbb{Z}_3; j \in \mathbb{Z}_2 \rangle.$$

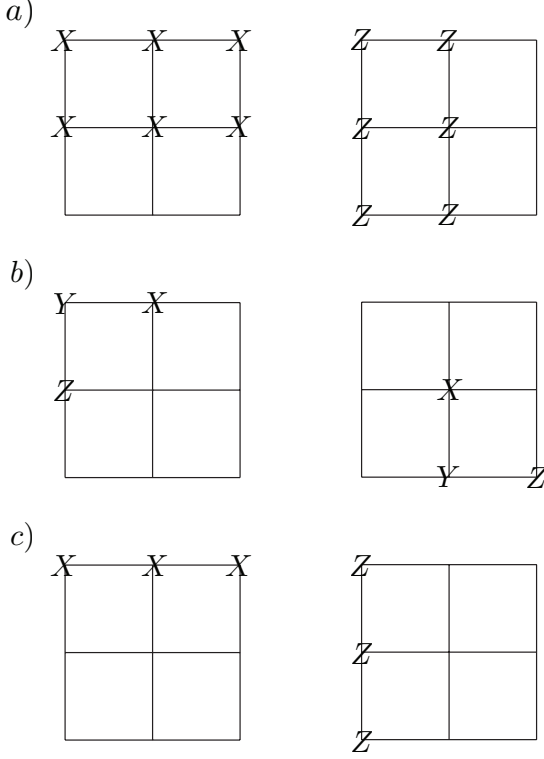


FIG. 16 Stabilizer structure for the  $\mathcal{C}(3,3)$  code. Fig a. gives two of the four stabilizers from the group  $\mathcal{S}$ . Fig. b. illustrates one of the four encoded Pauli operators from each subsystem defined with the Gauge group,  $\mathcal{T}$ . Fig. c. gives the two logical operators from the group  $\mathcal{L}$  which enact valid operations on the encoded qubit.

The third relevant subsystem is the logical space [Fig. 16c],  $\mathcal{L}$ , which can be defined through the logical Pauli operators

$$\mathcal{L} = \langle Z_{*,1}; X_{1,*} \rangle, \quad (81)$$

which when combined with  $\mathcal{S}$  form a non-Abelian group.

The stabilizer group  $\mathcal{S}$ , defines all relevant code states, i.e. *every* valid logical space is a +1 eigenvalue of this set. For the  $\mathcal{C}(3,3)$  code, there are a total of nine physical qubits and a total of four independent stabilizers in  $\mathcal{S}$ , hence there are five degrees of freedom left in the system which can house  $2^5$  logical states which are simultaneous eigenstates of  $\mathcal{S}$ . This is where the gauge group,  $\mathcal{T}$ , becomes relevant. As the gauge group is non-Abelian, there is no valid code state which is a simultaneous eigenstate of all operators in  $\mathcal{T}$ . However, if you examine closely there are a total of four encoded Pauli operations within  $\mathcal{T}$ . Fig 16b. illustrates two such operators. As all elements of  $\mathcal{T}$  commute with all elements of  $\mathcal{S}$  we can identify each of these four sets of valid “logical” qubits to be equivalent, i.e. we define  $\{|0\rangle_L, |1\rangle_L\}$  pairs which are eigenstates of  $\mathcal{S}$  and an abelian subgroup of  $\mathcal{T}$  and then ignore exactly what gauge group we are in (each of the four possible  $|0\rangle_L$  states can be used to store a single log-

ical qubit in the  $|0\rangle$  state, regardless of which particular  $|0\rangle_L$  gauge state we are in). Hence, each of these gauge states represent a subsystem of the code, with each subsystem logically equivalent.

The final group we considered is the logical group  $\mathcal{L}$ . This is the set of two Pauli operators which enact a logical  $X$  or  $Z$  gate on the encoded qubit *regardless* of the gauge choice and consequently represent true logical operations to our encoded space.

In a more formal sense, the definition of these three group structures allows us to decompose the Hilbert space of the system. If we let  $\mathcal{H}$  denote the Hilbert space of the physical system,  $\mathcal{S}$  forms an Abelian group and hence can act as a stabilizer set denoting subspaces of  $\mathcal{H}$ . If we describe each of these subspaces by the binary vector,  $\vec{e}$ , formed from the eigenvalues of the stabilizers,  $\mathcal{S}$ , then each subspace splits into a tensor product structure

$$\mathcal{H} = \bigoplus_{\vec{e}} \mathcal{H}_{\mathcal{T}} \otimes \mathcal{H}_{\mathcal{L}}, \quad (82)$$

where elements of  $\mathcal{T}$  act only on the subsystem  $\mathcal{H}_{\mathcal{T}}$  and the operators  $\mathcal{L}$  act only on the subsystem  $\mathcal{H}_{\mathcal{L}}$ . Therefore, in the context of storing qubit information, a logical qubit is encoded into the two dimensional subsystem  $\mathcal{H}_{\mathcal{L}}$ . As the system is already stabilized by operators in  $\mathcal{S}$  and the operators in  $\mathcal{T}$  act only on the space  $\mathcal{H}_{\mathcal{T}}$ , qubit information is only altered when operators in the group  $\mathcal{L}$  act on the system.

This formal definition of how subsystem coding works may be more complicated than the standard stabilizer codes shown earlier, but this slightly more complicated coding structure has significant benefits when we consider how error correction is performed. In general, to perform error correction, each of the stabilizers of the codespace must be checked to determine which eigenvalue changes have occurred due to errors. In the case of subsystem code this would appear to be problematic. The stabilizer group,  $\mathcal{S}$ , consist of qubit operators that scale with the size of the code. In our specific example, each of the  $X$  and  $Z$  stabilizers are six-dimensional (and in general, for a  $n_1 \times n_2$  lattice, the  $X$  stabilizers are  $2n_1$  dimensional and the  $Z$  stabilizers are  $2n_2$  dimensional). If techniques such as Shor’s method [Section XII] were used, we would need to prepare a large ancilla state to perform fault-tolerant correction, which would also scale linearly with the size of the code, this is clearly undesirable. However, due to the gauge structure of subsystem codes we are able to decompose the error correction procedure (AC07).

Each of the stabilizers in  $\mathcal{S}$  are simply the product of certain elements from  $\mathcal{T}$ , for example,

$$\begin{aligned} X_{1,1}X_{1,2}X_{1,3}X_{2,1}X_{2,2}X_{2,3} &\in \mathcal{S} \\ &= (X_{1,1}X_{2,1}) \cdot (X_{1,2}X_{2,2}) \cdot (X_{1,3}X_{2,3}) \in \mathcal{T}. \end{aligned} \quad (83)$$

Therefore if we check the eigenvalues of the three, 2-dimensional operators from  $\mathcal{T}$  we are able to calculate what the eigenvalue is for the 6-dimensional stabilizer. This decomposition of the stabilizer set for the code can

only occur since the decomposition is in terms of operators from  $\mathcal{T}$  which, when measured, has no effect on the logical information encoded within the system. In fact, when error correction is performed the gauge state of the system will almost always change based on the order in which the eigenvalues of the gauge operators are checked.

This exploitation of the gauge properties of subsystem coding is extremely beneficial for fault-tolerant designs for correction circuits. As the stabilizer operators can now be decomposed into multiple 2-dimensional operators, fault-tolerant circuits for error correction do not require any encoded ancilla states. Furthermore, if we decide to scale the code-space to correct more errors (increasing the lattice size representing the code) we do not require measuring operators with higher dimensionality. Fig 17 taken from Ref. (AC07) illustrates the fault-tolerant circuit constructions for Bacon-Shor subsystem codes. As each ancilla qubit is only coupled to two data

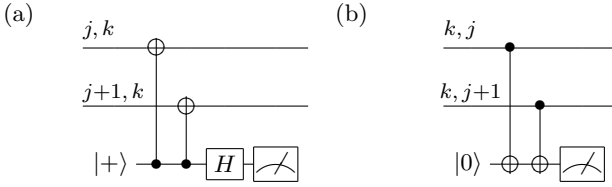


FIG. 17 (From Ref. (AC07)) Circuits for measuring the gauge operators and hence performing error correction for subsystem codes. Fig. a. measures, fault-tolerantly, the operator  $X_{j,k} X_{j+1,k}$  with only one ancilla. Fig. b. measures  $Z_{k,j} Z_{k,j+1}$ . The results of these two qubit parity checks can be used to calculate the parity of the higher dimensional stabilizer operators of the code.

qubits, no further circuit constructions are required to ensure fault-tolerance. The classical results from these 2-dimensional parity checks are then combined to calculate the parity of the higher dimensional stabilizer of the subsystem code.

A second benefit to utilizing subsystem codes is the ability to construct fault-tolerant circuits to perform dynamical code switching. When using more traditional error correction codes it is difficult, if not impossible, to fault-tolerantly switch between codes with different error correcting properties. The Steane  $[[7,1,3]]$  code is a single error correcting code for both  $X$  and  $Z$  channels. If during the operation of a quantum computer, the user wished to increase the error correcting power of their code to two errors in the  $X$  and  $Z$  channel they would first decode the quantum data and then re-encode with the higher distance code. This is clearly a non fault-tolerant procedure as any error occurring on the decoded information will cause catastrophic failure. Due to the general lattice structure of subsystem codes switching too and from higher order codes can be achieved without decoding and re-encoding information, allowing the user of the computer to dynamically adjust the error correction during the computation.

Figs. 18, 19 and 20, taken from Ref. (SEDH07) illus-

trates circuits to perform fault-tolerant switching from the  $\mathcal{C}(3,3)$  and  $\mathcal{C}(3,5)$  subsystem code. As noted before, the  $\mathcal{C}(3,3)$  is a single  $X$ , single  $Z$  error correcting code while the  $\mathcal{C}(3,5)$  is a single  $X$ , two  $Z$  error correcting code. We will not detail why these circuits successfully implement fault-tolerant code switching, instead we encourage readers to refer to Ref. (SEDH07) for further details.

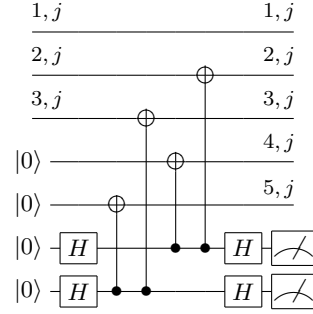


FIG. 18 (From Ref. (SEDH07)). Circuit to convert from the  $\mathcal{C}(3,3)$  subsystem code to the  $\mathcal{C}(5,3)$  code for one column,  $j$ , of the lattice structure of the code.

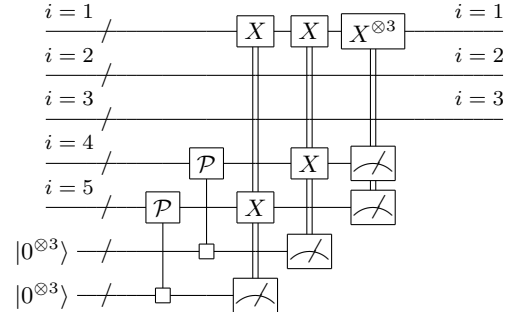


FIG. 19 (From Ref. (SEDH07)). Downconversion from the  $\mathcal{C}(5,3)$  code to the  $\mathcal{C}(3,3)$  code.  $\mathcal{P}$  is the gate sequence in Fig. 20.

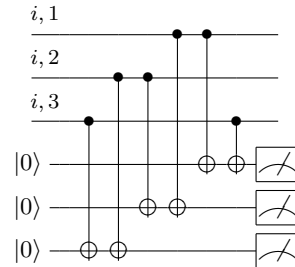


FIG. 20 (From Ref. (SEDH07))  $X$  parity measurement under  $\mathcal{C}(5,3)$  for one row,  $i$ , of the lattice structure.

## B. Topological Codes

A similar coding technique to the Bacon-Shor subsystem codes is the idea of topological error correction, first introduced with the Toric code of Kitaev in 1997 (Kit97). Topological coding is similar to subsystem codes in that the code structure is defined on a lattice (which, in general, can be of dimension  $> 2$ ) and the scaling of the code to correct more errors is conceptually straightforward. However, in topological coding schemes the protection afforded to logical information relies on the unlikely application of error chains which define non-trivial topological paths over the code surface.

Topological error correction is a complicated area of quantum error correction and fault-tolerance and any attempt to fairly summarize the field is not possible within this review. In brief, there are two ways of approaching the problem. The first is simply to treat topological codes as a class of stabilizer codes over a qubit system. This approach is more amenable to current information technologies and is being adapted to methods in cluster state computing (RHG07; FG08), optics (DFS<sup>+</sup>08; DMN08), ion-traps (SJ08) and superconducting systems (IFI<sup>+</sup>02). The second approach is to construct a physical Hamiltonian model based on the structure of the topological code. This leads to the more complicated field on anyonic quantum computation (Kit97). By translating a coding structure into a physical Hamiltonian system, excitations from the ground state of this Hamiltonian exhibit natural robustness against local errors (since their physical Hamiltonian symmetries reflect the coding structure imposed). Specifically, quasi-particles arising from a Hamiltonian approach to quantum codes exhibit fractional quantum statistics (they acquire fractional phase shifts when their positions are exchanged twice with other anyones, in contrast to Bosons or Fermions which always acquire  $\pm 1$  phase shifts). The unique properties of anyones therefore allow for natural, robust, error protection and anyone/anyone interactions are performed by rotating anyones around each other. However, the major issue with this model is that it relies on quasi-particle excitations that do not, in general, arise naturally. Although certain physical systems have been shown to exhibit anyonic excitations, most notably in the fractional quantum hall effect (NSS<sup>+</sup>08) the ability to first manufacture a reliable anyonic system in addition to reliably design and construct a large scale computing system based on anyons is a daunting task.

As there are several extremely good discussions of both anyonic (NSS<sup>+</sup>08) and non-anyonic topological computing (DKLP02; FSG08; FG08) we will not review any of the anyonic methods for topological computing and simply provide a brief example of one topological coding scheme, namely the surface code (BK01; DKLP02; FSG08). The surface code for quantum error correction is an extremely good error correction model for several reasons. As it is defined over a 2-dimensional lattice of

qubits it can be implemented on architectures that only allow for the coupling of nearest neighbor qubits (rather than the arbitrary long distance coupling of qubits in separate regions of the computer). The surface code also exhibits one of the highest fault-tolerant thresholds of any quantum error correction scheme, recent simulations estimate a threshold approaching 1% (RHG07). Finally, the surface code can correct problematic error channels such as qubit loss and leakage naturally.

The surface code, as with subsystem codes, is a stabilizer code defined over a 2-dimensional qubit lattice. Fig. 21 illustrates. We now identify each edge of the 2D lattice with a physical qubit. The stabilizer set consists of two types of operators, the first is the set of  $Z^{\otimes 4}$  operators which circle every lattice face (or plaquette). The second is the set of  $X^{\otimes 4}$  operators which encircle every vertex of the lattice. The stabilizer set is consequently generated by the operators,

$$A_p = \bigotimes_{j \in b(p)} Z_j, \quad B_v = \bigotimes_{j \in s(v)} X_j \quad (84)$$

where  $b(p)$  is the four qubits surrounding a plaquette and  $s(v)$  is the four qubits surrounding each vertex in the lattice and identity operators on the other qubits are implied. First note that all of these operators commute as any plaquette and vertex stabilizer will share either zero or two qubits. If the lattice is not periodic in either dimension, this stabilizer set completely specifies one unique state, i.e. for a  $N \times N$  lattice there are  $2N^2$  qubits and  $2N^2$  stabilizer generators. Hence this stabilizer set defines a unique multi-qubit entangled state which is generally referred to as a “clean” surface. Detailing exactly how this surface can be utilized to perform robust quantum computation is far outside the scope of this review and there are several papers to which such a discussion can be referred (RH07; RHG07; FSG08; FG08). Instead, we can quite adequately show how robust error correction is possible by simply examining how a “clean” surface can be maintained in the presence of errors. The  $X$  and  $Z$  stabilizer sets,  $A_p$  and  $B_v$  define two equivalent 2D lattices which are interlaced, Fig. 22, illustrates. If the total 2D lattice is shifted along the diagonal by half a cell then the operators  $B_v$  are now arranged around a plaquette and the operators  $A_p$  are arranged around a lattice vertex. Since protection against  $X$  errors are achieved by detecting eigenvalue flips of  $Z$  stabilizers and visa-versa, these two interlaced lattices correspond to error correction against  $X$  and  $Z$  errors respectively. Therefore we can quite happily restrict our discussion to one possible error channel, for example correcting  $X$  errors (since the correction for  $Z$  errors proceeds identically when considering the stabilizers  $B_v$  instead of  $A_p$ ).

Fig 23a. illustrates the effect that a single  $X$  error has on a pair of adjacent plaquettes. Since  $X$  and  $Z$  anti-commute, a single bit-flip error on one qubit in the surface will flip the eigenvalue of the  $Z^{\otimes 4}$  stabilizers on the two plaquettes adjacent to the respective qubit. As single qubit errors act to flip the eigenvalue of adjacent

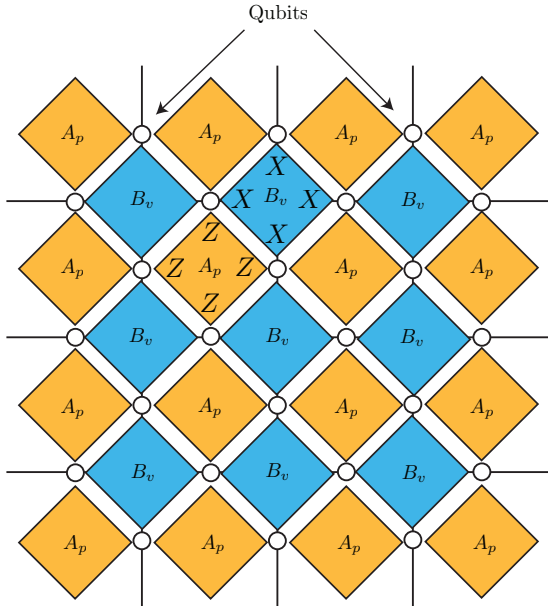


FIG. 21 General structure of the surface code. The edges of the lattice correspond to physical qubits. The four qubits surrounding each face (or plaquette) are  $+1$  eigenstates of the operators  $A_p$  while the four qubits surrounding each vertex are  $+1$  eigenstates of the operators  $B_v$ . If all eigenstate conditions are met, a unique multi-qubit state is defined as a “clean” surface.

plaquette stabilizers we examine how chains of errors affect the surface. Figs 23b. and Fig. 23c. examine two longer chains of errors. As you can see, if multiple errors occur, only the eigenvalues of the stabilizers associated with the ends of the error chains flip. Each plaquette along the chain will always have two  $X$  errors occurring on different boundaries and consequently the eigenvalue of the  $Z^{\otimes 4}$  stabilizer around these plaquettes will flip twice.

If we now consider an additional ancilla qubit which sits in the center of each plaquette and can couple to the four surrounding qubits, we can check the parity by running the simple parity circuit shown in Fig 24. If we assume that we initially prepare a perfect “clean” surface, we then, at some later time, check the parity of every plaquette over the surface. If  $X$  errors have occurred on a certain subset of qubits, the parity associated with the endpoints of error chains will have flipped. We now take this 2-dimensional *classical* data tree of eigenvalue flips and pair them up into the most likely set of error chains. Since it is assumed that the probability of error on any individual qubit is low, the most likely set of errors which reflects the eigenvalue changes observed is the minimum weight set (i.e. connect up all plaquettes where eigenvalues have changed into pairs such that the total length of all connections is minimized). This classical data processing is quite common in computer science and minimum weight matching algorithms such as the Blossom package (CR99; Kol08) have a running time polynomial in

the total number of data points in the classical set. Once this minimal matching is achieved, we can identify the likely error chains corresponding to the end points and correction can be applied accordingly.

The failure of this code is therefore dictated by error chains that cannot be detected through changes in plaquette eigenvalues. If you examine Fig 25, we consider an error chain that connects one edge of the surface lattice to another. In this case every plaquette has two associated qubits that have experienced a bit flip and no eigenvalues in the surface have changed. Since we have assumed that we are only wishing to maintain a “clean” surface, these error chains have no effect, but when one considers the case of storing information in the lattice, these types of error chains correspond to logical errors on the qubit (FSG08). Hence undetectable errors are chains which connect boundaries of the surface to other boundaries (in the case of information processing, qubits are artificial boundaries within the larger lattice surface) It should be stressed that this is a simplified description of the full protocol, but it does encapsulate the basic idea. The important thing to realize is that the failure rate of the error correction procedure is suppressed, exponentially with the size of the lattice. In order for a series of single qubit errors to be undetectable, they must form a chain connecting one boundary in the surface with another. If we consider an error model where each qubit experiences a bit flip, independently, with probability  $p$ , then an error chain of one occurs with probability  $p$ , error chains of weight two occur with probability  $O(p^2)$ , chains of three  $O(p^3)$  etc... If we have an  $N \times N$  lattice and we extend the surface by *one* plaquette in each dimension, then the probability of having an error chain connecting two boundaries will drop by a factor of  $p^2$  (two extra qubits have to experience an error one on each boundary). Extending an  $N \times N$  lattice by one plaquette in each dimension requires  $O(N)$  extra qubits, hence this type of error correcting code suppresses the probability of having undetectable errors exponentially with a qubit resource cost which grows linearly.

As we showed in Section X, standard concatenated coding techniques allow for an error rate suppression which scales with the concatenation level as a double exponential while the resource increase scales exponentially. For the surface code, the error rate suppression scales exponentially while the resource increase scales linearly. While these scaling relations might be mathematically equivalent, the surface code offers much more flexibility at the architectural level. Being able to increase the error protection in the computer with only a linear change in the number of physical qubits is far more beneficial than using an exponential increase in resources when utilizing concatenated correction. Specifically, consider the case where a error protected computer is operating at a logical error rate which is just above what is required for an algorithm. If concatenated error correction is employed, then adding another layer of correction will not only increase the number of qubits by an exponential amount,

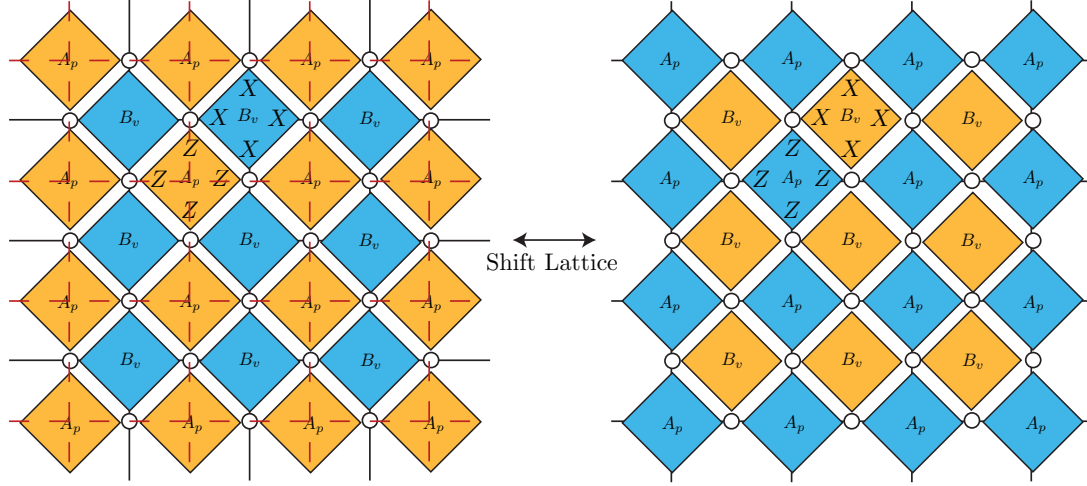


FIG. 22 The surface code imbeds two self similar lattices that are interlaced, generally referred to as the primal and dual lattice. Fig. a. illustrates one lattice where plaquettes are defined with the stabilizers  $A_p$ . Fig b. illustrates the dual structure where plaquettes are now defined by the stabilizer set  $B_v$ . The two lattice structures are interlaced and are related by shifting along the diagonal by half a lattice cell. Each of these equivalent lattices are independently responsible for  $X$  and  $Z$  error correction

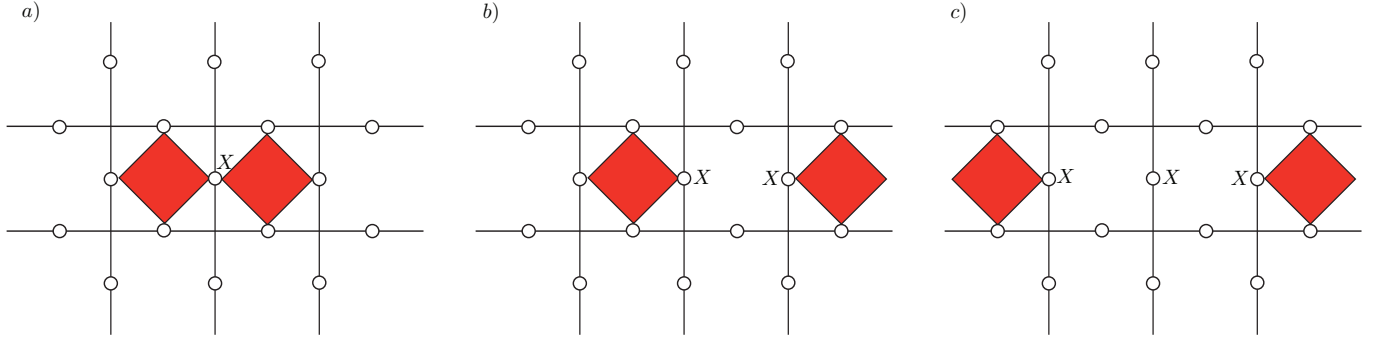


FIG. 23 Examples of error chains and their effect on the eigenvalues for each plaquette stabilizer. a). A single  $X$  error causes the parity of two adjacent cells to flip. b) and c). Longer chains of errors only cause the end cells to flip eigenvalue as each intermediate cell will have two  $X$  errors and hence the eigenvalue for the stabilizer will flip twice.

but it will also drop the effective logical error rate far below what is actually required. In contrast, if surface codes are employed, we increase the qubit resources by a linear factor and drop the logical error rate sufficiently for successful application of the algorithm.

We now leave the discussion regarding topological correction models. We emphasize again that this was a *very* broad overview of the general concept of topological codes. There are many details and subtleties that we have deliberately left out if this discussion and we urge the reader, if they are interested, to refer to the referenced articles for a much more thorough treatment of this topic.

## XV. CONCLUSIONS AND FUTURE OUTLOOK

This review has hopefully provided a basic introduction to some of the most important theoretical aspects of quantum error correction and fault-tolerant quantum computation. The ultimate goal of this discussion was not to provide a rigorous theoretical framework for QEC and fault-tolerance, but instead attempted to illustrate most of the important rules, results and techniques that have evolved out of this field.

We not only covered the basic aspects of QEC through specific examples, but also we have briefly discussed how physical errors influence quantum computation and how these processes are interpreted within the context of QEC. One of the more important aspects of this review is the discussion related to the stabilizer formalism, circuit synthesis and fault-tolerant circuit construction. Stabilizers are arguably the most useful theoretical formalism



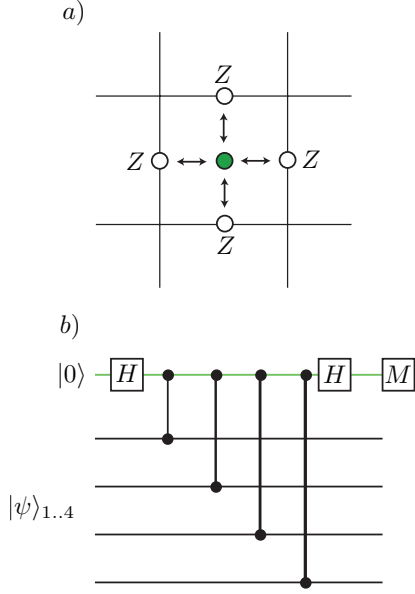


FIG. 24 a). Lattice structure to check the parity of a surface plaquette. An additional ancilla qubit is coupled to the four neighboring qubits that comprise each plaquette. b). Quantum circuit to check the parity of the  $Z^{\otimes 4}$  stabilizer for each surface plaquette.

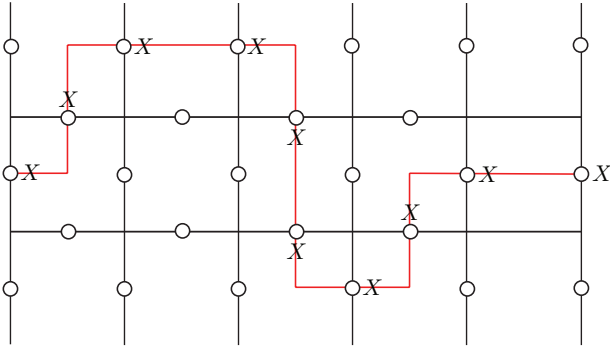


FIG. 25 Example of a chain of errors which do not cause any eigenvalue changes in the surface. If errors connect boundaries to other boundaries, the error correction protocol will not detect them. In the case of a “clean” surface, these error chains are invariants of the surface code. When computation is considered, qubit information are artificial boundaries within the surface. Hence if error chains connect these information qubits to other boundaries, logical errors occur.

in QEC as once it is sufficiently understood, most of the important properties of error correcting codes can be investigated and understood largely by inspection.

The study of quantum error correction and fault-tolerance is still an active area of QIP research. Although the library of quantum codes and error correction techniques are vast there is still a significant disconnect between the abstract framework of quantum coding and the more physically realistic implementation of error cor-

rection for large scale quantum information.

There are several future possibilities for the direction of quantum information processing. Even with the development of many of these advanced techniques, the physical construction and accuracy of current qubit fabrication is still insufficient to obtain any benefit from QEC. Many in the field now acknowledge that the future development of quantum computation will most likely split into two broad categories. The first is arguably the more physically realistic, namely few qubit application in quantum simulation.

Quantum simulation, i.e. using quantum systems to efficiently simulate other quantum systems was proposed by Richard Feynmann in the early 1980’s (Fey82) and was one of the primary motivations to the development of the field. In the ideal case, it is argued that having access to a quantum computer with on the order of 10-100 physical qubits could allow for simulating physical systems large enough to be impractical for current classical computers. If we limit our quantum array to the 100 qubit level, then even implementing active error correction techniques would not be desirable. Instead, higher quality fabrication and control as well as techniques in error avoidance (which require far less resources than error correction) would instead be used in order to lower effective error rates below what is required to run few qubit applications.

Beyond few qubit quantum simulation we move to truly large scale quantum computation, i.e. implementing large algorithms such as Shor on qubit arrays well beyond 1000 physical qubits. This would undoubtedly require active techniques in error correction. Future work needs to focus on adapting the many codes and fault-tolerant techniques to the architectural level. As we noted in section X.B, the implementation of QEC at the design level largely influences the fault-tolerant threshold exhibited by the code itself. Being able to efficiently incorporate both the actual quantum code and the error correction procedures at the physical level is extremely important when developing an experimentally viable, large scale quantum computer.

There are many differing opinions within the quantum computing community as to the future prospects for quantum information processing. Many remain pessimistic regarding the development of a million qubit device and instead look towards quantum simulation in the absence of active error correction as the realistic goal of quantum information. However, in the past few years, the theoretical advances in error correction and the fantastic speed in the experimental development of few qubit devices continues to offer hope for the near-term construction of a large scale device, incorporating many of the ideas presented within this review. While we could never foresee the possible successes or failures in quantum information science, we remain hopeful that a large scale quantum computer is still a goal worth pursuing.



## XVI. ACKNOWLEDGMENTS

The authors wish to thank A. M. Stephens, R. Van Meter, A.G. Fowler, L.C.L. Hollenberg, A. D. Greentree for helpful comments and acknowledge the support of MEXT, JST, the EU project QAP.

## References

- [ABO97] D. Aharonov and M. Ben-Or. Fault-tolerant Quantum Computation with constant error. *Proceedings of 29th Annual ACM Symposium on Theory of Computing*, page 46, 1997.
- [AC07] P. Aliferis and A.W. Cross. Subsystem fault tolerance with the Bacon-Shor code. *Phys. Rev. Lett.*, 98:220502, 2007.
- [AG04] S. Aaronson and D. Gottesman. Improved Simulation of Stabilizer Circuits. *Phys. Rev. A.*, 70:052328, 2004.
- [AJW<sup>+</sup>01] A. Aassime, G. Johansson, G. Wendin, R.J. Schoelkopf, and P. Delsing. Radio-Frequency Single-Electron Transistor as Readout Device for Qubits: Charge Sensitivity and Backaction. *Phys. Rev. Lett.*, 86:3376, 2001.
- [Ali07] P. Aliferis. PhD Thesis (Caltech), 2007.
- [ALKH02] D. Ahn, J. Lee, M.S. Kim, and S.W. Hwang. Self-Consistent non-Markovian theory of a quantum-state evolution for quantum-information-processing. *Phys. Rev. A.*, 66:012302, 2002.
- [APN<sup>+</sup>05] O. Astafiev, Yu. A. Pashkin, Y. Nakamura, T. Yamamoto, and J.S. Tsai. Quantum Noise in the Josephson Charge Qubit. *Phys. Rev. Lett.*, 93:267007, 2005.
- [ATK<sup>+</sup>08] T. Aoki, G. Takahashi, T. Kajiya, J. Yoshikawa, S.L. Braunstein, P. van Loock, and A. Furusawa. Quantum Error Correction Beyond Qubits. *arxiv:0811.3734*, 2008.
- [Avis87] A. Avizienis. *The Evolution of Fault-Tolerant Computing*. Springer-Verlag, New York, 1987.
- [Bac06] D. Bacon. Operator Quantum Error-Correcting Subsystems for self-correcting quantum memories. *Phys. Rev. A.*, 73:012340, 2006.
- [BBK03] A. Bririd, S.C. Benjamin, and A. Kay. Quantum error correction in globally controlled arrays. *quant-ph/0308113*, 2003.
- [BHPC03] N. Boulant, T.F. Havel, M.A. Pravia, and D.G. Cory. Robust Method for Estimating the Lindblad operators of a dissipative quantum process from measurements of the density operator at multiple time points. *Phys. Rev. A.*, 67:042322, 2003.
- [BK01] S.B. Bravyi and A.Y. Kitaev. Quantum codes on a lattice with boundary. *Quant. Computers and Computing*, 2:43, 2001.
- [BKD04] G. Burkard, R.H. Koch, and D.P. DiVincenzo. Multilevel quantum description of decoherence in superconducting qubits. *Phys. Rev. B.*, 69:064503, 2004.
- [BKSO05] S. Balensiefer, L. Kregor-Stickles, and M. Oskin. An Evaluation Framework and Instruction Set Architecture for Ion-Trap based Quantum Micro-architectures. *SIGARCH Comput. Archit. News*, 33(2):186, 2005.
- [BLWZ05] M.S. Byrd, D.A. Lidar, L.-A. Wu, and P. Zanardi. Universal leakage elimination. *Phys. Rev. A.*, 71:052301, 2005.
- [BM03] S.D. Barrett and G.J. Milburn. Measuring the Decoherence rate in a semiconductor charge qubit. *Phys. Rev. B.*, 68:155307, 2003.
- [BR01] H.-J. Briegel and R. Raussendorf. Persistent Entanglement in Arrays of Interacting Particles. *Phys. Rev. Lett.*, 86:910, 2001.
- [Bra98] S.L. Braunstein. Error Correction for continuous quantum variables. *Phys. Rev. Lett.*, 80:4084, 1998.
- [CG97] R. Cleve and D. Gottesman. Efficient Computations of Encodings for Quantum Error Correction. *Phys. Rev. A.*, 56:76, 1997.
- [CGJH05] V.I. Conrad, A.D. Greentree, D.N. Jamieson, and L.C.L. Hollenberg. Analysis and Geometric Optimization of Single Electron Transistors for Read-Out in Solid-State Quantum Computing. *Journal of Computational and Theoretical Nanoscience*, 2:214, 2005.
- [CR99] W. Cook and A. Rohe. Computing minimum-weight perfect matchings. *INFORMS Journal on Computing*, 11:138, 1999.
- [CRSS98] A.R. Calderbank, E.M. Rains, P.W. Shor, and N.J.A. Sloane. Quantum Error Correction via Codes Over GF(4). *IEEE Trans. Inform. Theory*, 44:1369, 1998.
- [CS96] A.R. Calderbank and P.W. Shor. Good Quantum Error-Correcting codes exist. *Phys. Rev. A.*, 54:1098, 1996.
- [DA07] D.P. DiVincenzo and P. Aliferis. Effective Fault-Tolerant Quantum Computation with slow measurement. *Phys. Rev. Lett.*, 98:020501, 2007.
- [DFS<sup>+</sup>08] S.J. Devitt, A.G. Fowler, A.M. Stephens, A.D. Greentree, L.C.L. Hollenberg, W.J. Munro, and K. Nemoto. Topological Cluster State Computation with Photons. *arxiv:0808.1782*, 2008.
- [DG97] L.-M. Duan and G.-C. Guo. Preserving Coherence in Quantum Computation by Pairing quantum Bits. *Phys. Rev. Lett.*, 79:1953, 1997.
- [DG98a] L.-M. Duan and G.-C. Guo. Prevention of dissipation with two particles. *Phys. Rev. A.*, 57:2399, 1998.
- [DG98b] L.-M. Duan and G.-C. Guo. Reducing decoherence in quantum computer-memory with all quantum bits coupling to the same environment. *Phys. Rev. A.*, 57:737, 1998.
- [DKLP02] E. Dennis, A. Kitaev, A. Landahl, and J. Preskill. Topological Quantum Memory. *J. Math. Phys.*, 43:4452, 2002.
- [DMN08] S.J. Devitt, W.J. Munro, and K. Nemoto. High Performance Quantum Computing. *arxiv:0810.2444*, 2008.
- [DN06] C.M. Dawson and M.A. Nielsen. The Solovay-Kitaev Algorithm. *Quant. Inf. Comp.*, 6(1):81, 2006.
- [DS96] D.P. DiVincenzo and P.W. Shor. Fault-Tolerant error correction with efficient quantum codes. *Phys. Rev. Lett.*, 77:3260, 1996.
- [DS00] M.H. Devoret and R.J. Schoelkopf. Amplifying Quantum Signals with the Single-Electron Transistor. *Nature (London)*, 406:1039, 2000.
- [DSO<sup>+</sup>07] S.J. Devitt, S.G. Schirmer, D.K.L. Oi, J.H. Cole, and L.C.L. Hollenberg. Subspace Confinement: How good is your Qubit? *New. J. Phys.*, 9:384, 2007.
- [DWM03] S. Daffer, K. Wódkiewicz, and J.K. McIver. Quantum Markov Channels for Qubits. *Phys. Rev. A.*, 67:062312, 2003.
- [EJ96] A. Ekert and R. Jozsa. Quantum Computation and Shor's Factoring Algorithm. *Rev. Mod. Phys.*, 68:733, 1996.
- [Fey82] R.P. Feynman. Simulating Physics with Computers.

- Int. J. Theor. Phys.*, 21:467, 1982.
- [FG08] A.G. Fowler and K. Goyal. Topological cluster state quantum computing. *arxiv:0805.3202*, 2008.
- [FLP04] P. Facchi, D.A. Lidar, and S. Pascazio. Unification of dynamical decoupling and the quantum Zeno effect. *Phys. Rev. A*, 69:032314, 2004.
- [Fow05] A.G. Fowler. PhD Thesis (Melbourne). *quant-ph/0506126*, 2005.
- [FSG08] A.G. Fowler, A.M. Stephens, and P. Groszkowski. High threshold universal quantum computation on the surface code. *arxiv:0803.0272*, 2008.
- [G83] P. Gács. Reliable computation with cellular automata. *Proc. ACM Symp. Th. Comput.*, 15:32, 1983.
- [Gar91] C.W. Gardiner. *Quantum Noise*, volume 56 of *Springer Series in Synergetics*. Springer -Verlag, Berlin ; New York, 1991.
- [GBP97] M. Grassl, Th. Beth, and T. Pellizzari. Codes for the quantum erasure channel. *Phys. Rev. A*, 56:33, 1997.
- [GC99] D. Gottesman and I.L. Chuang. Demonstrating the viability of Universal Quantum Computation using teleportation and single qubit operations. *Nature (London)*, 402:390, 1999.
- [GHSZ90] D.M. Greenberger, M.A. Horne, A. Shimony, and A. Zeilinger. Bell's theorem without inequalities. *Am. J. Physics*, 58:1131, 1990.
- [GHZ89] D.M. Greenberger, M.A. Horne, and A. Zeilinger. *Bell's theorem, Quantum, and Conceptions of the Universe*. Kluwer Academic, Dordrecht, 1989.
- [Got96] D. Gottesman. A Class of Quantum Error-Correcting Codes Saturating the Quantum Hamming Bound. *Phys. Rev. A*, 54:1862, 1996.
- [Got97] D. Gottesman. PhD Thesis (Caltech). *quant-ph/9705052*, 1997.
- [Got98] D. Gottesman. A theory of Fault-Tolerant quantum computation. *Phys. Rev. A*, 57:127, 1998.
- [Got02] D. Gottesman. An Introduction to Quantum Error Correction. *Quantum Computation: A Grand Mathematical Challenge for the Twenty-First Century and the Millennium*, ed. S. J. Lomonaco, Jr., pp. 221-235 (American Mathematical Society, Providence, Rhode Island, 2002), *quant-ph/0004072*, 2002.
- [Got09] D. Gottesman. An Introduction to Quantum Error Correction and Fault-Tolerant Quantum Computation. *arXiv:0904.2557*, 2009.
- [Gro97] L.K. Grover. Quantum Mechanics Helps in Searching for a Needle in a Haystack. *Phys. Rev. Lett.*, 79:325, 1997.
- [HMCS00] J.J. Hope, G.M. Moy, M.J. Collett, and C.M. Savage. Steady-State quantum statistics of a non-Markovian atom laser. *Phys. Rev. A*, 61:023603, 2000.
- [IFI<sup>+</sup>02] L.B. Ioffe, M.V. Feigel'man, A. Ioselevich, D. Ivanov, M. Troyer, and G. Blatter. Topologically protected quantum bits from Josephson junction arrays. *Nature (London)*, 415:503, 2002.
- [IHY85] N. Imoto, H.A. Haus, and Y. Yamamoto. Quantum nondemolition measurement of the photon number via the optical Kerr effect. *Phys. Rev. A*, 32:2287, 1985.
- [JFS06] S.P. Jordan, E. Farhi, and P.W. Shor. Error correcting codes for adiabatic quantum computation. *Phys. Rev. A*, 74:052322, 2006.
- [Kit97] A.Y. Kitaev. Quantum Computations: algorithms and error correction. *Russ. Math. Surv.*, 52(6):1191, 1997.
- [KL00] E. Knill and R. Laflamme. A Theory of Quantum Error-Correcting Codes. *Phys. Rev. Lett.*, 84:2525, 2000.
- [KLA<sup>+</sup>02] E. Knill, R. Laflamme, A. Ashikhmin, H. Barnum, L. Viola, and W.H. Zurek. Introduction To Quantum Error Correction. *Los Alamos Science*, 27:188, 2002.
- [KLM01] E. Knill, R. Laflamme, and G.J. Milburn. A Scheme for Efficient Quantum Computation with linear optics. *Nature (London)*, 409:46, 2001.
- [KLP05] D. Kribs, R. Laflamme, and D. Poulin. Unified and Generalized Approach to Quantum Error Correction. *Phys. Rev. Lett.*, 94:180501, 2005.
- [KLV00] E. Knill, R. Laflamme, and L. Viola. Theory of Quantum Error Correction for General Noise. *Phys. Rev. Lett.*, 84:2525, 2000.
- [KLZ96] E. Knill, R. Laflamme, and W.H. Zurek. Accuracy threshold for Quantum Computation. *quant-ph/9610011*, 1996.
- [Kni05] E. Knill. Quantum computing with realistically noisy devices. *Nature (London)*, 434:39, 2005.
- [Kol08] V. Kolmogorov. Blossom V: A new implementation of a minimum cost perfect matching algorithm. *Technical Report*: <http://www.adastral.ucl.ac.uk/vlad-kolm/papers/BLOSSOM5.html>, 2008.
- [LMPZ96] R. Laflamme, C. Miquel, J.P. Paz, and W.H. Zurek. Perfect Quantum Error Correcting Code. *Phys. Rev. Lett.*, 77:198, 1996.
- [LS98] S. Lloyd and J. E. Slotine. Analog Quantum Error Correction. *Phys. Rev. Lett.*, 80:4088, 1998.
- [LW03a] D.A. Lidar and K.B. Whaley. Decoherence-Free Subspaces and Subsystems. *quant-ph/0301032*, 2003.
- [LW03b] D.A. Lidar and L.-A. Wu. Encoded Recoupling and Decoupling: An Alternative to Quantum Error Correcting Codes, Applied to Trapped Ion Quantum Computation. *Phys. Rev. A*, 67:032313, 2003.
- [MCM<sup>+</sup>05] J.M. Martinis, K.B. Cooper, R. McDermott, M. Steffen, M. Ansmann, K.D. Osborn, K. Cicak, S. Oh, D.P. Pappas, R.W. Simmonds, and C.C. Yu. Decoherence in Josephson Qubits for Dielectric Loss. *Phys. Rev. Lett.*, 95:210503, 2005.
- [MCT<sup>+</sup>04] T. Metodiev, A. Cross, D. Thaker, K. Brown, D. Copsey, F.T. Chong, and I.L. Chuang. Preliminary Results on Simulating a Scalable Fault-Tolerant Ion Trap system for quantum computation. In *3rd Workshop on Non-Silicon Computing (NSC-3)*, online: [www.csif.cs.ucdavis.edu/metodiev/papers/NSC3-setso.pdf](http://www.csif.cs.ucdavis.edu/metodiev/papers/NSC3-setso.pdf), 2004.
- [MNBS05] W.J. Munro, K. Nemoto, R.G. Beausoleil, and T.P. Spiller. High-efficiency quantum-nondemolition single-photon-number-resolving detector. *Phys. Rev. A*, 71:033819, 2005.
- [MW84] G.J. Milburn and D.F. Walls. State reduction in quantum-counting quantum nondemolition measurements. *Phys. Rev. A*, 30:56, 1984.
- [NC00] M.A. Nielsen and I.L. Chuang. *Quantum Computation and Information*. Cambridge University Press, second edition, 2000.
- [Neu55] J. Von Neumann. Probabilistic logics and the synthesis of reliable organisms from unreliable components. *Automata Studies*, 43, 1955.
- [NSS<sup>+</sup>08] C. Nayak, S.H. Simon, A. Stern, M. Freedman, and S. Das Sarma. Non-Abelian anyons and topological quantum computation. *Rev. Mod. Phys.*, 80:1083, 2008.
- [POW<sup>+</sup>04] G.J. Pryde, J.L. O'Brien, A.G. White, S.D. Bartlett, and T.C. Ralph. Measuring a photonic qubit without destroying it. *Phys. Rev. Lett.*, 92:190402, 2004.
- [Pre98] J. Preskill. *Introduction To Quantum Computation*. World Scientific, Singapore, 1998.

- [PVK97] M.B. Plenio, V. Vedral, and P.L. Knight. Quantum Error Correction in the Presence of Spontaneous Emission. *Phys. Rev. A.*, 55:67, 1997.
- [RB01] R. Raussendorf and H.-J. Briegel. A One way Quantum Computer. *Phys. Rev. Lett.*, 86:5188, 2001.
- [RH07] R. Raussendorf and J. Harrington. Fault-tolerant quantum computation with high threshold in two dimensions. *Phys. Rev. Lett.*, 98:190504, 2007.
- [RHG05] T.C. Ralph, A.J.F. Hayes, and A. Gilchrist. Loss Tolerant Optical Qubits. *Phys. Rev. Lett.*, 95:100501, 2005.
- [RHG07] R. Raussendorf, J. Harrington, and K. Goyal. Topological fault-tolerance in cluster state quantum computation. *New J. Phys.*, 9:199, 2007.
- [SBF<sup>+</sup>06] T. Szkopek, P.O. Boykin, H. Fan, V.P. Roychowdhury, E. Yablonovitch, G. Simms, M. Gyure, and B. Fong. Threshold Error Penalty for Fault-Tolerant Computation with Nearest Neighbour Communication. *IEEE Trans. Nano.*, 5(1):42, 2006.
- [SDT07] K.M. Svore, D.P. DiVincenzo, and B.M. Terhal. Noise Threshold for a Fault-Tolerant Two-Dimensional Lattice Architecture. *Quant. Inf. Comp.*, 7:297, 2007.
- [SEDH07] A. Stephens, Z. W. E. Evans, S. J. Devitt, and L.C.L. Hollenberg. Subsystem Code Conversion. *arxiv:0708.3969*, 2007.
- [SFH08] A. Stephens, A.G. Fowler, and L.C.L. Hollenberg. Universal Fault-Tolerant Computation on bilinear nearest neighbor arrays. *Quant. Inf. Comp.*, 8:330, 2008.
- [Sho95] P.W. Shor. Scheme for reducing decoherence in quantum computer memory. *Phys. Rev. A.*, 52:R2493, 1995.
- [Sho96] P.W. Shor. Fault-Tolerant quantum computation. *Proc. 37th IEEE Symp. on Foundations of Computer Science.*, pages 56–65, 1996.
- [Sho97] P.W. Shor. Polynomial-Time algorithms for Prime Factorization and Discrete Logarithms on a Quantum Computer. *SIAM Journal of Sci. Statist. Comput.*, 26:1484, 1997.
- [SI05] A.M. Steane and B. Ibinson. Fault-Tolerant Logical Gate Networks for Calderbank-Shor-Steane codes. *Phys. Rev. A.*, 72:052335, 2005.
- [SJ08] R. Stock and D.F.V. James. A Scalable, high-speed measurement based quantum computer using trapped ions. *arxiv:0808.1591*, 2008.
- [ST98] J. Steinbach and J. Twamley. Motional Quantum Error Correction. *quant-ph/9811011*, 1998.
- [Ste96a] A.M. Steane. Error Correcting Codes in Quantum Theory. *Phys. Rev. Lett.*, 77:793, 1996.
- [Ste96b] A.M. Steane. Simple quantum error-correcting codes. *Phys. Rev. A.*, 54:4741, 1996.
- [Ste97a] A.M. Steane. Active Stabilization, Quantum Computation and Quantum State Synthesis. *Phys. Rev. Lett.*, 78:2252, 1997.
- [Ste97b] A.M. Steane. The Ion Trap Quantum Information Processor. *Appl. Phys. B*, 64:623, 1997.
- [Ste01] A.M. Steane. Quantum Computing and Error Correction. *Decoherence and its implications in quantum computation and information transfer, Gonis and Turchi, eds, pp.284-298 (IOS Press, Amsterdam, 2001), quant-ph/0304016*, 2001.
- [Ste02] A.M. Steane. Fast Fault-Tolerant filtering of quantum codewords. *quant-ph/0202036*, 2002.
- [Tof81] T. Toffoli. Bicontinuous extension of reversible combinatorial functions. *Math. Syst. Theory*, 14:13–23, 1981.
- [Unr95] W.G. Unruh. Maintaining Coherence in Quantum Computers. *Phys. Rev. A.*, 51:992, 1995.
- [VK03] L. Viola and E. Knill. Robust Dynamical Decoupling of Quantum Systems with Bounded Controls. *Phys. Rev. Lett.*, 90:037901, 2003.
- [VK05] L. Viola and E. Knill. Random Decoupling Schemes for Quantum Dynamical Control and Error Suppression. *Phys. Rev. Lett.*, 94:060502, 2005.
- [VKL99] L. Viola, E. Knill, and S. Lloyd. Dynamical Decoupling of Open Quantum Systems. *Phys. Rev. Lett.*, 82:2417, 1999.
- [VL98] L. Viola and S. Lloyd. Dynamical suppression of decoherence in two-state quantum systems. *Phys. Rev. A.*, 58:2733, 1998.
- [vL08] P. van Loock. A Note on Quantum Error Correction with Continuous Variables. *arxiv:0811.3616*, 2008.
- [VT99] D. Vitali and P. Tombesi. Using parity kicks for decoherence control. *Phys. Rev. A.*, 59:4178, 1999.
- [VWW05] J. Vala, K.B. Whaley, and D.S. Weiss. Quantum error correction of a qubit loss in an addressable atomic system. *Phys. Rev. A.*, 72:052318, 2005.
- [WBL02] L.-A. Wu, M.S. Byrd, and D.A. Lidar. Efficient Universal Leakage Elimination for Physical and Encoded Qubits. *Phys. Rev. Lett.*, 89:127901, 2002.
- [WZ82] W.K. Wothers and W.H. Zurek. A Single Quantum Cannot be Cloned. *Nature (London)*, 299:802, 1982.
- [Zan99] P. Zanardi. Symmetrizing evolutions. *Phys. Lett. A*, 258:77, 1999.
- [ZR97a] P. Zanardi and M. Rasetti. Error Avoiding Quantum Codes. *Mod. Phys. Lett. B.*, 11:1085, 1997.
- [ZR97b] P. Zanardi and M. Rasetti. Noisless Quantum Codes. *Phys. Rev. Lett.*, 79:3306, 1997.